Optical spectroscopy of $3d^7$ and $3d^8$ impurity configurations in a wide-gap semiconductor (ZnO:Co,Ni,Cu)

H.-J. Schulz and M. Thiede
Fritz-Haber-Institut der Max-Planck-Gesellschaft, Faradayweg 4-6, D-1000 Berlin 33, West Germany
(Received 5 May 1986)

Four emission bands have been studied at low temperatures with differently doped ZnO crystals. In the $Co^{2+}(d^7)$ ion, two transitions to the $^4A_2(F)$ ground state give rise to new luminescence bands, viz., starting from the $^4T_2(F)$ term (around 3600 cm^{-1}) and from the mixed $^4T_1(P),^2T_1(G),^2E(G)$ levels (around 15 100 cm^{-1}). Fine-structure and polarization properties of these transitions agree with conclusions on C_{3v} and spin-orbit splittings drawn from previous absorption data. An emission of ZnO:Ni near 6000 cm^{-1} is identified as the $^4T_2(F)\rightarrow{}^4A_2(F)$ transition of the $Ni^{3+}(d^7)$ ion in a trigonal environment. While the samples display the $Ni^{2+}(d^8)$ transmission spectrum, a charge-transfer process leads to a donor-type conversion of the center entailing the transient Ni^{3+} state. A similar mechanism is proposed to explain the emission of ZnO:Cu in the 5600—6900-cm^{-1} range. Its fine-structure and polarization behavior can be understood in terms of T_2-$^3T_2(F)\rightarrow A_1$-$^3T_1(F)$ transitions of a $Cu^{3+}(d^8)$ ion. Its occurrence is established in a model of one-electron configurations also covering the other known Cu transitions. The excitation spectrum presented is explained by a Tanabe-Sugano type of reasoning for the d^8 excited states which are reached in the $d^9\rightarrow d^8$ conversion.

I. INTRODUCTION

Among the II-VI compound semiconductors, ZnO has an exceptional position in several aspects. With ZnS it shares the property of a band gap large enough ($\bar{\nu}=27\,718$ cm^{-1} at $T=4.2$ K, cf. Ref. 1) to place it into the vicinity of insulating materials. High-lying Zn d bands and a mixing with the oxygen $2p$ states, which form predominantly the valence band, produce a negative spin-orbit splitting and a sequence of subbands which is $\Gamma_7,\Gamma_9,\Gamma_7$ at the center of the Brillouin zone and thus differs from that of the other direct-gap II-VI compound materials with C_{6v} structure. Various band-structure calculations are known.[2–5] The general properties of ZnO have recently been reviewed[6,7] and numerical data have been compiled as well.[8] To a lesser extent, impurity states of ZnO have been investigated. This follows from recent evaluations of absorption, reflection,[9] and luminescence processes.[1] The present study is intended to contribute to a further understanding of those electronic mechanisms which influence the optical characteristics of doped ZnO.

II. EXPERIMENTAL METHODS

High-resolution measurements have been carried out in the evacuated beam path of a 1-m grating monochromator (Jarrell-Ash). In absorption experiments, a halogen-W lamp or a globar have been used. In emission experiments, either a Xe high-pressure arc or an Ar cw laser provided the exciting radiation. Excitation spectra have been run on a setup whose core is a 0.3-m double-prism monochromator (Zeiss, Oberkochen). An approximately constant irradiance at changing wavelength is monitored by a split-beam signal which is fed to a motor controlling the slit widths. Commerical PbS or PbSe cells are employed to detect the chopped radiation in transmission or luminescence experiments, and the signals are processed by lock-in amplifiers. Repetitive scans are carried out by means of a step-motor drive, and the spectra are then stored and averaged.

Most of the measurements require cooling down to the liquid-He temperature range. He-bath cryostats equipped with optical windows are utilized for this purpose. By pumping on the He vessel, the temperature of the immersed sample can be reduced according to the pressure reached.

The experiments are carried out with single crystals grown from the vapor phase, most of them are needle shaped. A microprobe analysis commonly indicates the presence of Si. Several crystals were deliberately doped with Cu during growth.[10,11] However, some of the reported Cu properties are also found with other crystals which contain traces of copper without intentional Cu activation. Doping by Co or Ni has been carried out here by modifying a known annealing technique.[12]

III. LUMINESCENCE OF ZnO:Co

A quasiactivation of zinc oxide by cobalt is the occurrence of "Rinman's green" under a blowpipe flame.[13] The reaction is usually described as formation of a zinc-cobalt-(III) spinel, $ZnCo_2O_4$, or sometimes as that of cobalt-(II) zincate, $CoZn_2O_3$. In any case, the reaction product is present as a solid solution in ZnO.

Optical absorptions arising from transitions of the Co^{2+} ion in ZnO have been investigated by several authors.[14–18] No luminescent transitions related to Co have been identified so far. In a study of electrical properties,[19] at concentrations [Co] > 0.2 at. %, a new donor with approximately 240 cm^{-1} ionization energy appeared which

has been attributed to a Co complex. The presence of Co^{2+} pairs had earlier been derived from EPR spectra.[20]

Weakliem[16] has mainly studied the anisotropic ${}^4T_1(P) \leftarrow {}^4A_2(F)$ and ${}^4T_1(F) \leftarrow {}^4A_2(F)$ transitions of ZnO:$Co^{2+}(d^7)$ which are electric-dipole-allowed in T_d symmetry. The ${}^4T_2(F) \leftarrow {}^4A_2(F)$ absorption is forbidden in T_d and is merely mentioned to be observed[16] near $\bar{\nu}=3500$ cm^{-1}, while Pappalardo *et al.*[15] state a $\bar{\nu}=4140$ cm^{-1} (see Ref. 21 for units). This transition[22] which is of $\Gamma_1 \leftarrow \Gamma_2$ type in C_{3v} and still forbidden as such, becomes allowed, however, in the $\overline{C_{3v}}$ double group by spin-orbit interaction. Spin-forbidden transitions to mixed doublet states occur additionally near the ${}^4T_1(P)$ absorption. In a detailed study of the ${}^4T_2(F) \leftarrow {}^4A_2(F)$ absorption, Koidl[18] notes the positions of the transitions to the Γ_4 and Γ_5,Γ_6 spin-orbit components of ${}^4\Gamma_1(C_{3v})$-${}^4T_2(F)$ from the Γ_5,Γ_6 and Γ_4 spin-orbit components of the ${}^4\Gamma_2(C_{3v})$-${}^4A_2(F)$ ground state as 3635.9, 3630.8, 3617.3, and 3611.6 cm^{-1}, respectively. These spectra mainly reflect the 18.9-cm^{-1} splitting of the excited state by spin-orbit interaction. The corresponding splitting of the ground state is obtained as 5.4 cm^{-1} and agrees with the zero-field splitting $2D=5.5$ cm^{-1} derived from low-temperature EPR data.[20]

With ZnO crystals which were deliberately doped with cobalt, a luminescence is now observed at low temperature near 3600 cm^{-1} (Fig. 1). On doubling the spectral resolution, the main peak near 3610 cm^{-1} is resolved into a doublet at 3610.6; 3616.3 cm^{-1} (right-hand part of Fig. 1). At a spectral slit width of about 1 cm^{-1}, the main peak has about 3-cm^{-1} width at half height. The splitting of 5.7 cm^{-1} approximately matches that of the main absorption lines.[18] The shift of 1 cm^{-1} in the absolute positions could be due to a deviating calibration or, less likely, to self-absorption in the luminescence lines. As in the spectra of Koidl, the low-energy component in the doublet has an approximately fivefold strength compared with the high-energy line. The polarization properties of these lines are as well in accordance with his findings: The 3611 cm^{-1} main line ($\Gamma_5,\Gamma_6 \leftrightarrow \Gamma_5,\Gamma_6$) is preferentially polarized with $\mathbf{E}||\mathbf{c}$ whereas the 3616-cm^{-1} line ($\Gamma_5,\Gamma_6 \leftrightarrow \Gamma_4$) shows a preference for the orientation $\mathbf{E}\perp\mathbf{c}$. Koidl also states a partial violation of the polarization selection rules and attributes this observation to mixing of the components of the excited state, mediated by internal strain.

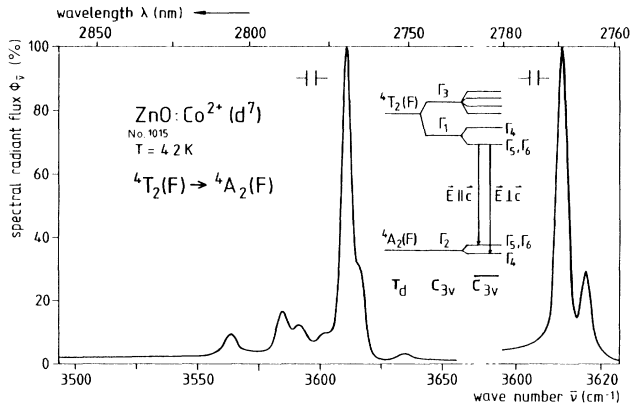

FIG. 1. Emission spectrum of a ZnO:Co crystal (No. 1015) at $T=4.2$ K. Excitation by xenon lamp in the range $10\,000 \lesssim \bar{\nu} \lesssim 30\,000$ cm^{-1}. The spectrum is due to the transition ${}^4T_2(F) \rightarrow {}^4A_2(F)$ of the $Co^{2+}(d^7)$ ion. The main peak in the survey scan (left-hand part) is plotted with higher resolution in the right-hand part. Inset: Splitting scheme of the relevant energy levels of a d^7 configuration and interpretation of the no-phonon doublet. Here, preferential directions of polarization are indicated.

Shifted by about 25 cm^{-1} towards lower energy, another emission doublet is resolved as 3585;3592 cm^{-1}, followed by a small peak at 3563 cm^{-1}. These subsidiary structures disappear on warming, their origin is still uncertain. They may be related to reduced acoustic phonons as observed with dynamic Jahn-Teller coupling[23] but for ZnO:Co there is no evidence yet of this interaction.[18] Also, centers in a disturbed environment could be liable to a low-energy shift with respect to the isolated centers. The displacement of the lines would in this case indicate the presence of strain fields, possibly related to pairing.[20] Phonon-assisted transitions shifted by several 100 cm^{-1} as expected from LO or TO coupling could not be discerned in the region down to $\bar{\nu}=2700$ cm^{-1}.

A high-energy satellite near 3635 cm^{-1} has a distance from the main emission line which is likely to result from an addition of the 6 cm^{-1} splitting in the ground state and the 19 cm^{-1} splitting[18] in the ${}^4\Gamma_1$-${}^4T_2(F)$ excited state. Indeed, this maximum corresponds to the 3635.9-cm^{-1} absorption line[18] and indicates a thermalization in the initial state of the luminescence transition. An expected companion near 3631 cm^{-1} is not resolved in the 4.2-K emission spectrum. However, near $T \simeq 15$ K, the spectral radiant flux is increased in this spectral region, and a doublet structure with about 6-cm^{-1} splitting is recorded. Even the polarization properties of these "hot lines" match those of the respective absorption transitions.[18]

The properties of the ZnO:Co emission depicted in Fig. 1 leave no doubt that one is dealing with the transitions inverse to the ${}^4T_2(F)$ absorption of Co^{2+}. Although these corresponding absorption structures cannot be detected with our weakly activated samples, some of the allowed stronger Co^{2+} absorptions are, viz., the ${}^4T_1(F)$ structure near 6000 cm^{-1} and the combined ${}^4T_1(P)$, spin-doublet bands near 15 400 cm^{-1}.

The ZnO:Co crystals used also exhibit the well-known green emission band of ZnO:Cu (cf., Ref. 1). On its low-energy, tail another new emission structure is now detected which is evidently related to ${}^4T_1(P),{}^2T_1(F),{}^2E(G) \rightarrow {}^4A_2(F)$ internal Co^{2+} transitions. The luminescence spectrum is dominated by a peak near $\bar{\nu}=15\,130$ cm^{-1} (Fig. 2, left-hand part). Comparing this emission at improved resolution with the transmission spectrum (Fig. 2, right-hand part) reveals an emission doublet at 15 134.8;15 129.1 cm^{-1} with a coinciding absorption at 15 134.8 cm^{-1} and indicates that the luminescence near 15 200 cm^{-1} is still subject to self-absorption by Co^{2+} internal transitions.

The edge of the emission near 15 140 cm^{-1} corresponds to Koidl's 15 142-cm^{-1} absorption line.[18] Evidently the high-energy component of the emission doublet is curtailed by self-absorption. The low-energy line is displayed

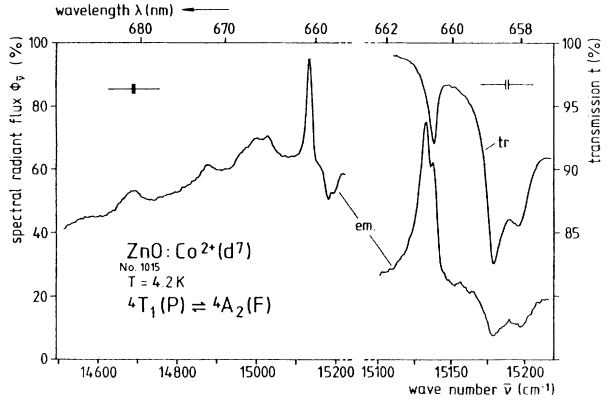

FIG. 2. Emission spectrum of a ZnO:Co crystal (No. 1015) at $T=4.2$ K in the range of the ${}^4T_1(P),{}^2T_1(G),{}^2E(G)\rightarrow{}^4A_2(F)$ transitions of $Co^{2+}(d^7)$. Excitation with 27488 and 28482 cm^{-1} argon laser lines. The nonphonon line in the survey scan (left-hand part) is resolved into a doublet (right-hand part) and compared with the transmission spectrum in the same region. The polarization is almost total with $\mathbf{E}\perp\mathbf{c}$ for both emission and transmission.

in emission only, in absorption merely a tail is noticeable there. The splitting of the emission doublet is with 5.7 cm^{-1} close to the value of 5.1 cm^{-1} given by Koidl. The reason of the deviating absolute positions is not yet clear. In accordance with the published absorption spectra, an almost total polarization of the luminescence in $\mathbf{E}\perp\mathbf{c}$ orientation is noted.

The new luminescence is again interpreted as an inversion of Koidl's respective absorption transitions. According to Koidl,[18] a mixing of the ${}^4T_1(P)$ components with those of ${}^2G$ is involved. Following this reasoning, the initial state of the emission should be a Γ_4-${}^2E(G)$ level which is reached after relaxation in the excited state. The emission doublet would thus represent the trigonal ground state splitting into Γ_5,Γ_6 and Γ_4, as in the emission of Fig. 1. While the value of 5.7 cm^{-1} for the splitting matches the value determined from the ${}^4T_2(F)\rightarrow{}^4A_2(F)$ transition (cf., Fig. 1), the $\mathbf{E}\perp\mathbf{c}$ polarization found for the whole doublet in Koidl's absorption study and in the present emission measurement does not conform with this conclusion. Koidl traces the polarization behavior to the C_{3v} splitting of ${}^3T_1(P)$, claiming that the Γ_3 component comes out lower than Γ_2 and that the electric-dipole transitions are governed by the Γ_3-${}^3T_1(P)\leftrightarrow\Gamma_2$-${}^4A_2(F)$ selection rule which indeed calls for $\mathbf{E}\perp\mathbf{c}$. The current results show no thermalization in the emission doublet near 4 K. This supports the assumption of the splitting taking place in the ground state. The polarization would thus indicate $\Gamma_4\rightarrow\Gamma_4$ or $\Gamma_5,\Gamma_6\rightarrow\Gamma_5,\Gamma_6$ transitions in $\overline{C_{3v}}$. The still unsatisfying understanding of the ${}^4T_1(P)$ components (and their nearby doublet descendants) resembles the situation[24–26] for the ${}^3T_1(P)$ levels of d^8. ZnO:Co is nevertheless another instance where the recovery of a center from a higher excited state is radiative as well as that from the lowest one. Examples have been given for internal and recombination transitions of $3d$ impurities.[27–30]

Although excitation spectra of the Co^{2+} luminescence bands have not been obtained yet, the observation of a preferential response of the 3600-cm^{-1} emission to blue excitation may signify a relationship with Weakliem's absorption tail rising near 22000 cm^{-1}. It could indicate the photoionization threshold for the process $Co^{2+}(d^7)+h\nu\rightarrow Co^{3+}(d^6)+e_{CB}^-$, if analogy with CdSe:Co (Ref. 31) is assumed. In that case, the liberated conduction electron could be recaptured by the photoionized Co^{3+} via excited Co^{2+} states which then return radiatively to the Co^{2+} ground state. At all events, in view of the emission presented in Fig. 2, the proposal[32] that ${}^4T_1(P)$ and the nearby doublet levels are degenerate with the conduction band is to be questioned. A relation can, however, be presumed of this low-T emission with a room-temperature electroluminescence band of ZnO:Co electrodes in electrolytes,[33] centered around 14200 cm^{-1}.

To summarize, the substitutional Co_{Zn}^{2+} ion[34] is confirmed to be subject to an axial field of C_{3v} symmetry while the spin-orbit splittings of the initial and final states of the ${}^4T_2(F)\rightarrow{}^4A_2(F)$ emission can be estimated as 19 and 6 cm^{-1}, respectively. Koidl's conclusions about the Co^{2+}-level scheme[18] are supported as far as the respective states are involved in the transitions treated here. This includes the exceptional role of the ZnO:Co^{2+} system with respect to the absence of Jahn-Teller interactions in the orbital singlets Γ_1 and Γ_2 of C_{3v}.

IV. LUMINESCENCE OF ZnO:Ni

The earlier investigations of the absorption properties of ZnO:Ni (Refs. 14, 16, and 35) have been continued in several studies dealing with details of internal transitions of $Ni^{2+}(d^8)$, viz., ${}^3T_1(P)\leftarrow{}^3T_1(F)$ (Refs. 17 and 24), and ${}^3T_2(F)\leftarrow{}^3T_1(F)$ (Ref. 36). An emission of ZnO:Ni has early been discovered[37] with polycrystalline samples at $T=90$ K. The luminescence spectrum had the form of a broad ($\Delta\bar{\nu}_{1/2}\simeq 300$ cm^{-1}) band peaking near 5900 cm^{-1} with a subsidiary maximum near 5400 cm^{-1}. This emission was tentatively interpreted[37] as the ${}^3T_2(F)\rightarrow{}^3T_1(F)$ transition of Ni^{2+} although the respective absorption was known[16,35] to take place in the (4200—4500)-cm^{-1} range. Two of the reported features of this luminescence are well worth mentioning: (i) a large decay constant of about 100 μs which even increased on warming the sample from 90 to 160 K, (ii) the necessity of stimulating the specimen with $\bar{\nu}\gtrsim 22000$ cm^{-1} during excitation in the ${}^3A_2(F)$ absorption band (8000—11000 cm^{-1}). The supposition that this stimulation could involve processes of the type $Ni^{2+}(d^8)+h\nu\rightarrow Ni^{3+}(d^7)+e_{CB}^-$, prompted speculations[38] on internal d^7 transitions causing the 5900-cm^{-1} infrared emission.

The present work aims at settling the origin of this Ni luminescence by measurements with ZnO single crystals. The low-temperature emission spectrum recorded (Fig. 3, left-hand part) displays a fairly sharp no-phonon structure near $\bar{\nu}=6092$ cm^{-1} and, apart from some minor elevations, a peak at $\bar{\nu}=5500$ cm^{-1}. At higher resolution (right-hand part of Fig. 3), a doublet structure is revealed in the main transition, with two components of opposite preferential polarization at 6090.5 cm^{-1} ($\mathbf{E}\|\mathbf{c}$) and

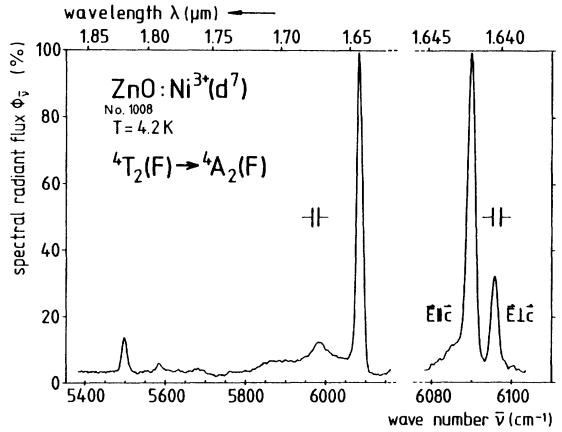

FIG. 3. Emission spectrum of a ZnO:Ni crystal (No. 1008). Excitation by xenon lamp in the range $20\,000 \leq \bar{\nu} \leq 30\,000$ cm^{-1}. The main peak in the survey scan at $T=4.2$ K (left-hand part) is resolved into a doublet in the right-hand part, taken at $T \simeq 2$ K. Here, preferential directions of polarization are indicated. The spectrum is assigned to the transition $^4T_2(F) \rightarrow {}^4A_2(F)$ of the Ni^{3+}(d^7) ion. See inset of Fig. 1 for details of d^7 level splitting and for polarization rules.

6096.2 cm^{-1} (E⊥c). The width at half height of the main line with $\Delta\bar{\nu}_{1/2}=2$ cm^{-1} is in Fig. 3 still limited by the slit width. With narrower slits, $\Delta\bar{\nu}_{1/2}=1.3$ cm^{-1} has been estimated.

There is no doubt that the structured emission of Fig. 3 is the one of Ref. 37 except for the improved resolution. Using the exact position of this transition, the idea[37] that a transition is neither involved to the ground state of Ni^{2+}, nor between any of the excited Ni^{2+} levels, is soon validated. Moreover, a search for an additional emission in the $^3T_2(F) \rightarrow {}^3T_1(F)$ range was unsuccessful. This is the more surprising as in ZnS (Refs. 23 and 29) and ZnSe (Refs. 23,39,40) this very process is known to be radiative. However, the overall shape of the spectrum in Fig. 3 differs clearly from the much more strongly phonon-coupled $^3T_2(F) \rightarrow {}^3T_1(F)$ emission in ZnS and ZnSe. Also, the characteristic satellites are missing, which are related to multiplet components of the Ni^{2+} ground state.[41].

The contour of the luminescence in question resembles indeed the known emissions of Ni$^+$(d^9) (Refs. 23 and 42) or of Co^{2+}(d^7) (Ref. 43) in ZnS. The prevalence of the no-phonon lines seems to rule out band-impurity transitions and an implication of associated centers as well. The connection with Ni doping having been demonstrated in Ref. 37 and also by our own preparations, the present considerations concentrate on the isolated Ni$^+$(d^9) and Ni^{3+}(d^7) ions. The necessity of an additional stimulation[37] favors the assumption of a light-induced change of a charge state anyway, and earlier experiments experiments have established that Ni^{3+} in ZnO (Ref. 44) as well as Ni^{3+} and Ni$^+$ in ZnS (Ref. 45) can be detected by photosensitive EPR signals. Some preference for the d^7 configuration over d^9 is derived from the notice that Ni$^+$ has not been detected by EPR in ZnO (cf., Ref. 46). Even more convincing is, of course, the similarity of the spectra in Figs. 1 and 3. In fact, our interest in ZnO:Co^{2+} was raised by the previous occupation with ZnO:Ni.

Assuming the transitions of Fig. 3 to arise from the Ni^{3+}(d^7) configuration which is isoelectronic to Co^{2+}(d^7), the level scheme of the inset of Fig. 1 can be used for the description of the transitions involved. The main doublet is likewise assigned to the transitions from the lower Γ_5,Γ_6 level of $\Gamma_1(C_{3v})$-$^4T_2(F)$ into the spin-orbit components Γ_5,Γ_6 and Γ_4 of the $\Gamma_2(C_{3v})$-$^4A_2(F)$ Ni^{3+} ground state. The emission lines at 6096.2 cm^{-1} (E⊥c) and 6090.5 cm^{-1} (E∥c) thus determine the splitting between Γ_5,Γ_6 and Γ_4 in the Ni^{3+} ground state as 5.7 cm^{-1}. This value compares favorably not only with the corresponding splitting in the Co^{2+} ion (cf. Sec. III) but also with the estimate[44] $2D=\lambda(g_{\parallel}-g_{\perp}) \simeq 4$ cm^{-1} which was merely based on the Ni^{3+} free-ion value for the many-electron spin-orbit parameter λ. The general symmetry interdiction of $T_2 \rightarrow A_2$ electric-dipole transitions is eventually in agreement with the weakness of the 6090 cm^{-1} luminescence as well as with the extremely slow decay noted by the inventors.[37]

Endeavors to find an inverse absorption transition proved to be in vain, therefore, a statement cannot be made on the corresponding splitting in the excited state. The absence of such absorption is, of course, expected, due to instability of the photogenerated Ni^{3+} centers. Consequently, this nonappearance is a further proof of the proposed interpretation. On warming the crystal from 4 K, an overall broadening of the faint emission spectrum is observed, but this time no "hot lines" could be resolved which would have been a clue to the fine structure of the initial state. The annexed structures in the emission spectrum at energies below the no-phonon line (NPL) are entirely comprehensible in terms of lattice phonons coupling to the transition. The shifts read from Fig. 3 compare favorably with published data on ZnO critical point phonons,[47–52] cf., Sec. VII C. The conclusion drawn for ZnO:Co^{2+}, viz., that the lower levels of the d^7 configuration are not liable to Jahn-Teller interaction, is thus corroborated with ZnO:Ni^{3+}.

Due to the low intensity of the luminescence in Fig. 3, an excitation spectrum could not be obtained. An additional complication arises with many of the Ni-activated samples in that they contain Cu additionally, thus displaying the emission discussed in Sec. V. In these cases, the Ni spectrum is superimposed onto the Cu luminescence so that a separation by filters becomes impossible. With such ZnO:Cu,Ni crystals, either one of these impurity emissions can be favored by suitable excitation: Whereas on "blue" illumination the Ni luminescence is preferred, "red" excitation would advance the Cu emission. In accordance with Ref. 37, an excitation of the Ni^{3+} emission is nevertheless feasible in the 10 000-cm^{-1} region (cf. Sec. VI B). In this event, an additional sensitizing illumination leads to a higher gain if this stimulation is effected by the green Ar-laser line ($\simeq$19 400 cm^{-1}) compared to use of the blue line ($\simeq$22 000 cm^{-1}). The stimulating radiation is expected to change the ionization state of nickel from Ni^{2+} to Ni^{3+}. The threshold for this process, read as approximately 21 000 cm^{-1} from Ref. 37, marks the onset of transitions involving the center and either the conduction or the valence band, cf. Sec. VI. The

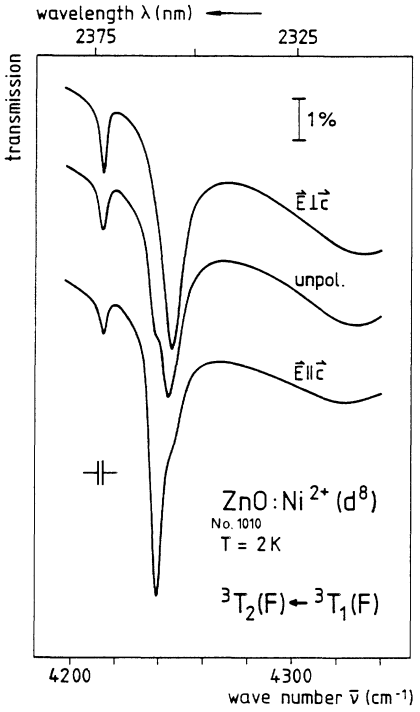

FIG. 4. Transmission spectrum of a ZnO:Ni crystal (No. 1010) at $T=2$ K, featuring the principal structures in the ${}^3T_2(F)\leftarrow{}^3T_1(F)$ transition of the $Ni^{2+}(d^8)$ ion. The curves have been shifted in the vertical direction such as to avoid overlap. The 1% bar provides a calibration measure both for the polarized and the unpolarized spectra.

absence of a ${}^3T_1(P)\rightarrow{}^3T_1(F)$ Ni^{2+} luminescence in the observed spectra can be due to $Ni^{2+}\rightarrow Ni^{3+}$ processes which are induced by the minimum energy required for excitation of this Ni^{2+} transition. Unidentified broad red emission bands of ZnO (cf., Ref. 1) however, display a high-energy rising point near 14 900 cm^{-1}, i.e., just in the expected spectral range.

As mentioned above, the ZnO:Ni crystals used have also been studied for their absorption spectra. These are determined by the known Ni^{2+} transitions. As an example, the main lines of the ${}^3T_2(F)\leftarrow{}^3T_1(F)$ absorption[36] are given (Fig. 4). The assignment of these lines is still not indisputable. For simplicity, the interpretation of Ref. 36 is adopted here. With this reservation, the 4215-cm^{-1} transition is terminating in $\Gamma_3(C_{3v})$-T_1-${}^3T_2(F)$, and the stronger polarized lines at 4240 cm^{-1} (**E**||**c**) and 4247 cm^{-1} (**E**⊥**c**), in Γ_1 and $\Gamma_3(C_{3v})$ of T_2-${}^3T_2(F)$, respectively. Their splitting of 7 cm^{-1} compares well with the value of 6 cm^{-1} given by Kaufmann *et al.*[36] The influence of the trigonal field is thus of comparable magnitude for ${}^3T_2(F)$ of Ni^{2+} and for ${}^4A_2(F)$ of Ni^{3+}.

V. LUMINESCENCE OF ZnO:Cu

While the existence of an infrared emission of ZnO:Cu had been asserted[53] as early as 1958, it was not until 1969 that its properties were studied in some detail.[54] The most striking feature of this luminescence is the position of the NPL at $\bar{\nu}=6890$ cm^{-1} which is shifted towards higher energy from the main absorption doublet at $\bar{\nu}=5821;5784$ cm^{-1}. The absorption[16,55–57] has been known for quite some time as being due to the ${}^2E(D)\leftarrow{}^2T_2(D)$ transition of Cu_{Zn}^{2+}. Its doublet splitting of 37 cm^{-1} is caused by the Γ_4 and Γ_5,Γ_6 components of ${}^2E$ in C_{3v}. A definite identification[58] of this absorption in terms of $Cu^{2+}(d^9)$ transitions was finally possible by means of a ^{63}Cu, ^{65}Cu isotope splitting and a Zeeman experiment which yielded the anisotropic g factors known from EPR.

Since the spectral position of the Cu emission and also its Zeeman g factors[54,59] are different from those of the described Cu^{2+} absorption, it has been inferred[1] that the luminescence is not related to isolated substitutional Cu_{Zn}^{2+}. The same conclusion was reached when lately this ir emission of ZnO:Cu was rediscovered.[60] With the aforementioned Ni^{3+} emission, the Cu luminescence shares the absence of any inverse absorption. The 5821;5784 cm^{-1} absorption doublet does, however, appear in the form of dips in the emission of more strongly Cu-doped crystals.[59,60]

If the relationship of the luminescence in question with copper is to be maintained, as suggested by the unanimous preparational experience of all previous authors, then, in principle, the substitutional Cu could form part of a complex with some other impurity or imperfection of the lattice. Indications of Cu-Cu pairs have been observed[10,61] with ZnO. In that case, a lowering of symmetry from C_{3v} to C_3 or C_s should influence the emission spectrum. A complicated model recently proposed[62] which is based on a magneto-optical study of the main emission line, postulates Cu_{Zn}^{+} Zn_i^{+} pairs with a preservation of the C_{3v} symmetry of the substitutional lattice site. In the excited state of this double-donor—acceptor associate, a three-particle system Cu_{Zn}^{2+}-e^--Zn_i^{+} would emerge and a variety of auxiliary assumptions is necessary to explain the Zeeman pattern and intensities. Moreover, the responsible Cu could be incorporated on interstitial sites. No evidence has been obtained, however, from EPR studies[54,58,63] of ZnO:Cu that Cu_i (cf., Ref. 64) is a common type of center in this material.

More consequent seems to be, therefore, the hypothesis of a charge state different from Cu^{2+} involved in this emission process. This idea has not only been triggered by the analogy with the treated $Ni^{2+}\rightleftarrows Ni^{3+}$ system (Sec. IV) but also by recent findings of $Cu^{2+}\rightleftarrows Cu^{3+}$ transitions[65] in ZnS. The improbability of the existence of Cu^{3+} ions in binary semiconductors claimed recently[62] is therefore questionable. The hypothesis of an at least transient existence of Cu^{3+} in ZnO shall be examined in the light of experimental data.

Cu^{3+} has a d^8 configuration and is thus isoelectronic with the Ni^{2+} ion. Its ${}^3T_1(F)$ ground state in a T_d crystal field is split by spin interactions, with an A_1 component lowest in energy. With a C_{3v} perturbation, a Γ_1 ground state would emerge. For the splitting of the ${}^3T_2(F)$ cubic crystal-field term which is next to the ground state, the sequence A_2,E,T_2,T_1 (ordered by decreasing energy) has been derived[36] for ZnO:Ni^{2+} from ${}^3T_2(F)\leftarrow{}^3T_1(F)$ polarized absorption data and a concomitant Jahn-Teller calculation which gives the correct level positions in C_{3v}. The

inverse transition ${}^3T_2(F) \rightarrow {}^3T_1(F)$ is luminescent with the Ni^{2+} ion in ZnS (Ref. 29), ZnSe (Ref. 39), and CdSe (Ref. 31). For cubic ZnS:Ni^{2+}, the longstanding question whether the T_1 or the T_2 spin-orbit component of ${}^3T_2(F)$ is lowest has been solved recently[66] by a combined absorption-emission experiment which places T_2 above T_1 by about 2 cm^{-1}.

The first clue to an interpretation of the emission structure of ZnO:Cu (Fig. 5) in terms of ${}^3T_2(F) \rightarrow {}^3T_1(F)$ transitions of a Cu^{3+} center is provided by the polarization properties[59] of its main lines. The dominating line (E_I) at $\bar{\nu} \simeq 6887$ cm^{-1} has a preferential polarization with $\mathbf{E} \| \mathbf{c}$ but only a degree of polarization of 0.2, approximately. The ground state being Γ_1 in C_{3v}, a $\Gamma_1 \rightarrow \Gamma_1$ transition is suggested by the electric-dipole selection rules. The excited state therefore seems to be the $\Gamma_1(C_{3v})$ component of T_2-${}^3T_2(F)$ (Fig. 6). The Γ_3 component expected close to it would give rise to the accompanying thermalized satellite[59,60] shifted to higher energy by about 4 cm^{-1}. This would explain the incomplete polarization of the main line and would fix the trigonal Γ_3, Γ_1 splitting of T_2-${}^3T_2(F)$ to $\Delta\bar{\nu} \simeq 4$ cm^{-1} which compares favorably with the 6 cm^{-1} found[36] with ZnO:Ni^{2+}. The transition $T_1 \rightarrow A_1$ is not allowed by electric-dipole rules in T_d, thus absence of T_1-${}^3T_2(F) \rightarrow A_1$-${}^3T_1(F)$ emission is not surprising here, although an interplay of T_1 and T_2 components in the excited state is conceivable as will be discussed later on.

The present experiments yield a shift of 4.0 cm^{-1} for the high-energy satellite of E_I and render for the first time its pronounced polarization with $\mathbf{E} \perp \mathbf{c}$ at $T = 4$ K. This fact supports the proposed interpretation as a thermalized Γ_3-T_2-${}^3T_2(F) \rightarrow \Gamma_1$-$A_1$-${}^3T_1(F)$ transition of d^8. An emission spectrum taken at $T = 77$ K (Ref. 59) re-

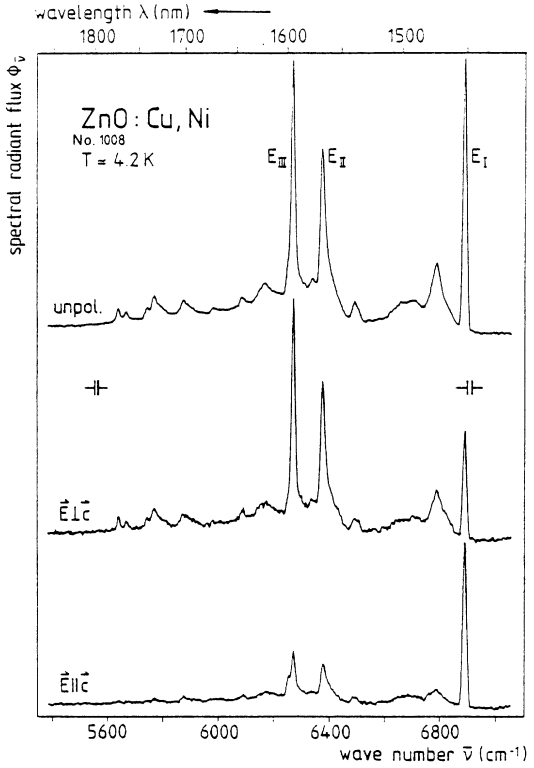

FIG. 5. Near-infrared emission of a ZnO:Cu,Ni crystal (No. 1008) at $T \simeq 4.2$ K. The polarized spectra have been shifted vertically to clear overlap. Excitation range: $7400 \leq \Delta\bar{\nu} \leq 12\,500$ cm^{-1}. The spectrum has been recorded by means of a cooled PbS detector ($T \simeq 240$ K), no corrections have been performed for the spectral sensitivity.

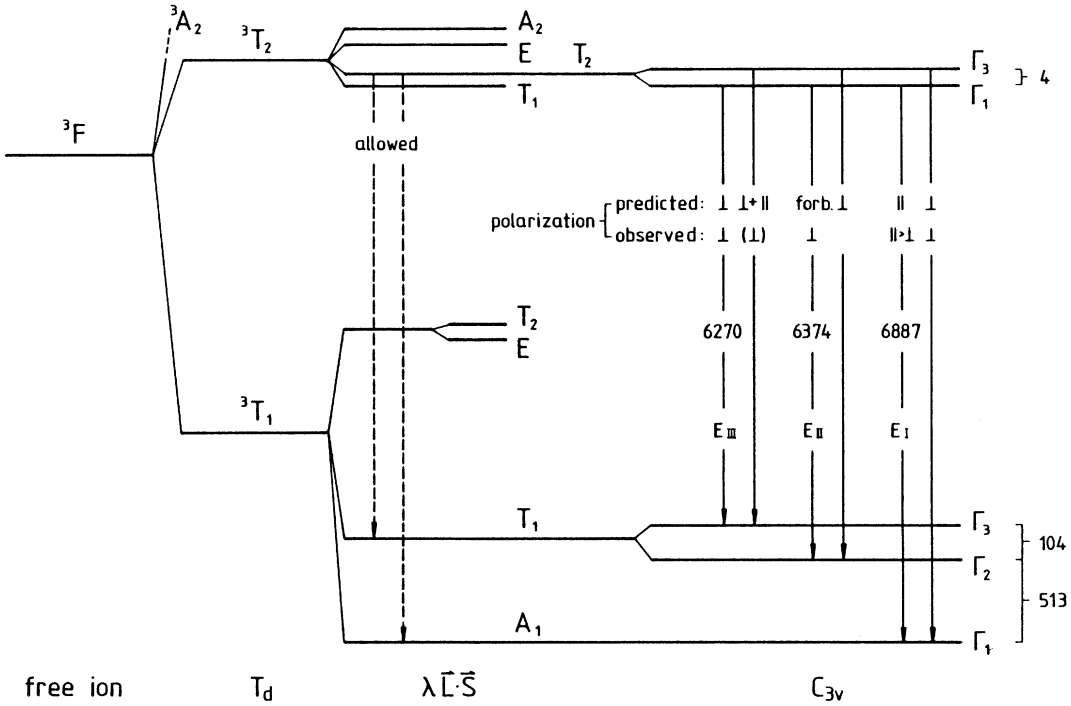

FIG. 6. Scheme of the relevant energy levels of a d^8 electron configuration in C_{3v} symmetry, giving rise to the Cu^{3+} internal transitions suggested to cause the near-infrared emission of ZnO:Cu. All indicated differences are given as wave numbers (in cm^{-1}).

veals a reversal of the polarization behavior in the broadened E_I region. The peak is now preferentially polarized with $\mathbf{E}\perp\mathbf{c}$ (degree nearly 0.3). Since at this temperature the Γ_3 component of T_2-$^3T_2(F)$ has over 90% of the population of the lower Γ_1 component, this is another evidence in favor of the d^8 model.

From magnetic susceptibility measurements[67] with ZnO:Ni^{2+}, the levels Γ_3 (at 260 cm^{-1}) and Γ_2 (at 160 cm^{-1}), both being trigonal components of T_1-$^3T_1(F)$, are to be expected above the Γ_1 ground state. The next prominent structure (E_{II}) in the emission spectrum (Fig. 5) is at 6374 cm^{-1}, polarized strongly with $\mathbf{E}\perp\mathbf{c}$. The asymmetrical shape of this peak is conspicuous. Experiments with increased resolution ($\Delta\bar{\nu}\simeq 2$ cm^{-1}) again reveal a thermalized precursor line here which is, however, apparent as a shoulder only and cannot clearly be connected with a definite polarization. Both observations are probably due to superposition of phonon-assisted background orginating from E_I. The transition $\Gamma_1\rightarrow\Gamma_2$ being forbidden in C_{3v}, the line E_{II} probably borrows its intensity from the $\Gamma_3\rightarrow\Gamma_2$ transition which then determines the polarization as well. The lower intensity of this transition as compared with E_I and E_{III} is nevertheless apparent in Fig. 5 and in the $T=1.6$ K spectrum of Ref. 62.

Finally, the 6270 cm^{-1} line (E_{III}) would correspond to Γ_1-T_2-$^3T_2(F)\rightarrow\Gamma_3$-$T_1$-$^3T_1(F)$, which is polarized accordingly with $\mathbf{E}\perp\mathbf{c}$. Again, a high-resolution experiment clearly indicates a shoulder in a distance of 4 cm^{-1} which is temperature-sensitive in the (2—4)-K range. The experimental evidence is thus in favor of a model with a common initial split state for the transitions E_I, E_{II}, and E_{III}. The resulting Γ_3,Γ_2 splitting $\Delta\bar{\nu}\simeq 104$ cm^{-1} of the T_1 ground multiplet component indeed conforms with the mentioned figures for ZnO:Ni^{2+}. The high position of these levels, viz., 617 and 513 cm^{-1}, respectively, above the Γ_1 ground state seems to point towards a comparatively small or negligible Jahn-Teller interaction in the $^3T_1$ ground-state manifold.

The overall structure of the luminescence spectrum is thus in qualitative concord with the general fine-structure splitting of a d^8 electron configuration. Some further comments on quantitative aspects of this interpretation may be appropriate. The distances of the main lines which are assigned to transitions terminating in the $^3T_1$ ground multiplet refer to its splitting by combined spin-orbit, spin-spin, and trigonal crystal-field effects. Previous estimates[16] predict a totaled splitting of about 1100 cm^{-1} for ZnO:Ni^{2+} while empirical arguments[23,41] yield $\simeq$1000 cm^{-1} for ZnS:Ni^{2+} and $\simeq$780 cm^{-1} for ZnSe:Ni^{2+}. The rough agreement of the distances in the ZnO:Cu emission with these data should indicate spin-orbit effects in the order of those predicted by static crystal field theory, unlike the behavior of the $^3T_2$ multiplet of ZnO:Ni^{2+} which is subject to quenching of spin-orbit interaction by dynamic Jahn-Teller effect.[36] Negligible Jahn-Teller interaction has also been proposed recently[65] for a copper associate, the "Cu-M" center in ZnS. Emission transitions from $^3T_2(F)$ to T_2,E-$^3T_1(F)$ have not been idenfitied here. There are, however, some small peaks in the 5700-cm^{-1} region—even with a separation of 100 to 110 cm^{-1}, the magnitude expected for a trigonal splitting of T_2-$^3T_1(F)$—which could possibly correspond to these anticipated transitions, cf. Sec. VI C.

A remarkable observation in comparing various ZnO:Cu spectra, even those in different publications of the same group of authors,[60,62] is a distinct variation in the line positions. The deviations are smaller for E_I but stronger for the second and third main lines, e.g., 6272 cm^{-1} (Ref. 60) or 6290 cm^{-1} (Ref. 62) for E_{III}. Not only are the variations larger than comprehensible with calibration errors, the mutual distances of the peaks are at variance, too. There is no definite explanation to this fact, yet a changing influence of the environment is well conceivable. This point seems to favor the proposition[62] of a preferential pairing of the radiating ion with some neighbored partner, e.g., a donor. This assumption of an associated luminescence center is still consistent with the Cu^{3+} model proposed here.

The ZnO:Cu emission (Fig. 5) has been studied with one of the ZnO:Ni crystals used previously (cf., Fig. 3). Indeed, this luminescence is detectable not only with samples that are deliberately Cu-doped but with nearly all ZnO crystals studied. It is felt, however, that this occurrence indicates the ubiquitous presence of copper rather than a participation of various activator ions. Appearance of the Cu emission often seems to be favored by long-time annealing procedures. No decisive deviations in the spectra of differently doped crystals could be secured.

The spectrum of Fig. 5 presents a number of maxima in addition to the peaks discussed so far, many of them explicable as phonon-assisted transitions. Regarding the separation from the respective "no-phonon" line (NPL) and in some cases the shape of the structures as indication of their origin, the following conclusions can be drawn: E_I and E_{III} have satellites in a distance of 100 cm^{-1}, probably due to TO (Γ) coupling. An analogous replica of E_{II} may be concealed in the broadened high-energy wing of E_{III}. LA interaction with E_I seems to prevail in the (6600—6700)-cm^{-1} range. TO(Γ) satellites in a distance of 393 ± 1 cm^{-1} are clearly discernible for E_I, E_{II}, and E_{III}. This energy value corresponds closely to the arithmetic average over TO$(E_1)_{\perp c}$ and TO$(A_1)_{\parallel c}$ (Ref. 8).

The main peaks E_{II} and E_{III} have previously[60] been interpreted as optical or local mode satellites of E_I. The shifts of 513 and 617 cm^{-1} versus E_I exceed significantly, however, the respective phonon energies (cf., Ref. 8). They neither match known bulk-phonon combinations nor surface modes of ZnO. Therefore, it seems more plausible to assume electronic transitions for E_{II} and E_{III} as proposed above. The missing "genuine" phonon satellites of E_I could be masked in the rise of the unsymmetrical structures E_{II} and E_{III}. They are, however, not apparent in the region of the phonon-assisted transitions of either E_{II} or E_{III}. But there are also no second-order satellites of E_{II} or E_{III} in the characteristic distances of 513 or 617 cm^{-1}. Subsidiary peaks at 5870 and 5763 cm^{-1} may represent, however, $\simeq$505 cm^{-1} satellites of E_{II} and E_{III}, i.e., an interplay of modes deviating from the phonon energies proper. And a peak at 6343 cm^{-1} could signal the participation of a $\simeq$540 cm^{-1} LO_2 phonon[52,68] in the E_I transition, thus corroborating the 538 cm^{-1} satellites identified in the $^2E(D)\leftarrow{}^2T_2(D)$ absorption of

ZnO:$Cu^{2+}(d^9)$. In addition to the mentioned structures near 5700 cm^{-1}, the maximum near 6090 cm^{-1} is related to another electronic transition (Fig. 5). It is also displayed in Ref. 60 and represents the principal line of $Ni^{3+}(d^7)$, cf., Fig. 3. Finally, from the viewpoint of polarization properties, an interpretation of E_{II} and E_{III} as phonon satellites of E_I appears to be doubtful as well. Selection rules for phonon-coupled transitions can be derived by a subgroup induction procedure.[69] They imply that a $\Gamma_1 \rightarrow \Gamma_1(C_{3v})$ transition such as E_I (according to Ref. 62 and likewise to the Cu^{3+} model presented here) would couple with all Γ-point phonons in $\mathbf{E} \perp \mathbf{c}$ polarization. But as these are not clearly discernible in the emission, their participation still remains open here.

An important means for conclusions on the identity of the levels involved in the emission process is provided by Zeeman experiments. Heinze[59] resolved four components of line E_I in $\mathbf{B} \perp \mathbf{c}$ orientation while West *et al.*[62] discriminate up to five. These latter authors deduce a zero-field splitting $\delta \simeq 1.3$ cm^{-1} and conclude that the excited state is a spin doublet close to a higher spin quartet while a doublet ground state is involved. They develop a fairly complex explanation in terms of a $[Cu_{Zn}^{+}(d^{10})]'[Zn_i^{+}(s^1)]^{\cdot}$ axial pair ground state and a $[Cu_{Zn}^{2+}(d^9)]^{\times} e'[Zn_i^{+}(s^1)]^{\cdot}$ excited state. The symbols $\times$, $\cdot$ and $'$ denote neutral, positive, and negative effective charge, respectively, of the constituent in square brackets. The excited state is thus a three-particle system with a $^1\Gamma_1$ and a higher-lying $^3\Gamma_1$ state split off by exchange interaction between the bound electron e' and the Cu core, both these states being derived from the ground $\Gamma_4(\overline{C_{3v}})$ state of Cu^{2+}. The Zeeman components of all these levels (including the ground state) are then claimed to be doubled by coupling to the donor electron. This model essentially fails to explain the 4-cm^{-1} high-energy satellite of line E_I and can, only together with auxiliary assumptions of magnetic mixing and a second-order spin-flip process, account for the observed anomalous switching of intensity between Zeeman components.

The Cu^{3+} model proposed here invokes with its $\Gamma_3, \Gamma_1 \rightarrow \Gamma_1$ transitions (cf., Fig. 6) primarily a triplet$\rightarrow$singlet type of splitting. If, however, the idea is retained of a coupling to a donor electron in the excited state, a sixfold splitting will result which is in principle sufficient for producing the five observed Zeeman lines, part of which are being thermalized anyway. Also, a mixing-in of the mentioned T_1-$^3T_2(F)$ components close to the initial state of the emission (cf., ZnS:Ni^{2+}, Ref. 66) may interfere. Before a more elaborate model can be developed along these lines of thought, high-resolution Zeeman measurements with polarized light are desired. Even a synthesis of the present Cu^{3+} model with the idea of a preferential donor-acceptor pairing is conceivable, still without the majority of auxiliary propositions necessitated by the model of Ref. 62.

VI. CHARGE EXCHANGE OF TRANSITION METAL IONS

A. General considerations

As details of the excitation mechanisms leading to the Co^{2+} emissions (Figs. 1 and 2) are not settled yet, internal or charge transfer processes come into question. No experiments are known which would prove the existence of a charge state of cobalt in ZnO other than Co^{2+}. There is, however, a photoabsorption threshold[16] (cf. Sec. III), and dark conductivity[70] as well as photoconductivity[32] indicate donor behavior, i.e., generation of $Co^{3+}(d^6)$ whose stability was recently proposed by means of a cluster model.[71] This can be contrasted to ZnS where in addition to the known Co^{2+} optical transitions those of $Co^{+}(d^8)$ have been identified.[72]

Nickel and copper are here found to emit in a charge state differing from the effectively neutral, double-positive ion that replaces Zn substitutionally. The three-fold positive state involved would point to a donorlike behavior of both these ions, e.g.,

$$[Ni^{2+}]^{\times} \rightleftarrows [Ni^{3+}]^{\cdot} + e'_{CB} \ . \tag{1}$$

Donor character has indeed been suggested for Ni as well. A thermal ionization energy of 290 cm^{-1} has been derived[70] while other authors have placed the Ni^{2+} ground state about 18 000 cm^{-1} below the conduction band.[33]

In comparable host-dopant systems, there is strong evidence of an ambipolar character of centers formed by incorporation of $3d$ transition metals,

$$[Ni^{3+}]^{\cdot} + e'_{CB} \rightleftarrows [Ni^{2+}]^{\times} \rightleftarrows e^{\cdot}_{VB} + [Ni^{+}]' \ . \tag{2}$$

Interactions of these impurities with both conduction and valence band have, therefore, to be taken into account here. Particularly under above-gap excitation, the initial state, e.g., $[Ni^{2+}]^{\times}$, may at first bind an exciton X, before this state would decay according to the scheme (2). The Umladung (1) could, in principle, be effected by hole participation,

$$e^{\cdot}_{VB} + [Ni^{2+}]^{\times} \rightleftarrows [Ni^{3+}]^{\cdot} \ . \tag{3}$$

In contrast to reactions (1) and (2), there is evidently no Coulomb attraction involved between the partners on the left-hand side of (3). Moreover, to proceed to the right, this process requires an additional hole-generating mechanism, e.g., the acceptor-type conversion of the right-hand side in (2). Together with the symmetry considerations to follow, these implications may be responsible for the notion that processes (3) cannot be verified here. The shape of a photoionization spectrum can be derived from assumptions on the wave functions involved.[73] For uniaxial crystals the absorption spectrum was deduced under the influence of configuration interaction.[74]

The ZnO lattice belongs to the crystallographic class C_{6v}, while a substitutional impurity site has the symmetry of the point group C_{3v}. To examine the selection rules for transitions between an impurity and one of the host lattice bands, the compatibility rules between these groups[22] are used.[31] Only transitions involving the Γ point of the Brillouin zone are considered. This is a simplification already, since for cubic semiconductors the L minimum has been reasoned[75] to be more important than Γ. The irreducible representation (irrep) of the conduction band minimum, Γ_7 of the double group $\overline{C_{6v}}$, corresponds to Γ_4 of $\overline{C_{3v}}$. The same reasoning yields Γ_4 for the maximum of the A valence band, but a subband B split off by spin-

orbit interaction is only 39 cm^{-1} below A, its irrep $\Gamma_9(\overline{C_{6v}})$ being split into $\Gamma_5+\Gamma_6$ in $\overline{C_{3v}}$. The ground states of the relevant impurity configurations d^8, d^9, and d^{10} are classified in $\overline{C_{3v}}$ by the irreps Γ_1, Γ_4, and Γ_1, respectively. The operator of the electric-dipole moment transforms as Γ_1 for $\mathbf{E}\|\mathbf{c}$ orientation and as Γ_3 for $\mathbf{E}\perp\mathbf{c}$. The results of the application of selection rules are uniform with respect to valence and conduction band since they both belong to the same irrep for this material. It turns out that $d^7 \leftrightarrow d^8$ and $d^9 \leftrightarrow d^{10}$ are forbidden for donor-type as well as for acceptor-type transitions. This outcome is still true if the Γ_9 valence subband is considered. On the other hand, $d^8 \leftrightarrow d^9$ conversions are allowed in both directions of polarization, for both the valence and conduction bands.

B. Charge conversion of nickel

According to the preceding section, the generation of the $Ni^{3+}(d^7)$ center from $Ni^{2+}(d^8)$ by virtue of light is a process which is forbidden under electric-dipole selection rules. The excitation of $3d^7$ internal transitions starting from a d^8 electron configuration is, however, enabled by a sequence of processes which will evolve via an excited state of Ni^{3+},

$$[Ni^{2+}(d^8)]^{\times} + h\nu(d^8/d^{7*}) \rightarrow [Ni^{3+}(d^{7*})]^{\cdot} + e'_{CB} , \quad (4a)$$

$$[Ni^{3+}(d^{7*})]^{\cdot} \rightarrow [Ni^{3+}(d^7)]^{\cdot} + h\nu(d^7) , \quad (4b)$$

$$[Ni^{3+}(d^7)]^{\cdot} + e'_{CB} \rightarrow [Ni^{2+}(d^8)]^{\times} . \quad (4c)$$

The excitation process (4a) is now allowed for some of the excited states (Γ_1,Γ_3) under electric-dipole selection rules. The deexcitation and radiative recombination (4b) is governed by the usual laws for internal transitions (cf. inset of Fig. 1). The reaction (4c) involves the electric-dipole-forbidden $d^7 \leftrightarrow d^8$ donor-type recombination which indeed turns out to be nonradiative.

The (7500–12000)-cm^{-1} Ni^{3+} excitation band[37] which approximately covers the range of the $^4T_1(F) \leftarrow {}^4A_2(F)$ absorption of the isoelectronic $Co^{2+}(d^7)$ ion is, therefore, rather a result of (4a)-type processes. In other words, the transition energy involved is neither due to Ni^{2+} nor to Ni^{3+} internal transitions but is comprised of internal [probably $^4T_2(F) \leftarrow {}^4A_2(F)$] and photoionization contributions, as will be exemplified with Cu in Sec. VI C.

C. Charge conversion of copper

The symmetry rules allow a formation of Cu^{3+} (d^8) from $Cu^{2+}(d^9)$ in ZnO under optical irradiation. The processes which lead to an excitation of d^8 luminescence starting from the stable presence of Cu^{2+} in this material are studied by means of excitation spectroscopy. The excitation spectrum (Fig. 7) of the photoluminescence depicted in Fig. 5 is in a principal concordance with earlier observations.[1,54,60] Yet not all of its features have been secured so far, and a convincing interpretation has not been offered by the previous authors.

The peaks at 10400 and 12200 cm^{-1} are about five times higher than those at 17000 and 18800 cm^{-1}. The double-peak contour in both regions is noteworthy. LO

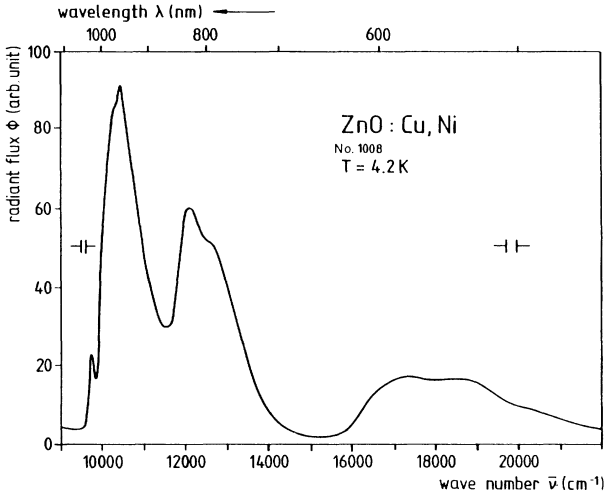

FIG. 7. Excitation spectrum of the infrared luminescence of a ZnO:Ni,Cu crystal (No. 1008) at $T=4.2$ K. Detected emission range: $3000 \leq \bar{\nu} \leq 7200$ cm^{-1}. The spectral slit width is $\Delta\bar{\nu} \lesssim 300$ cm^{-1}.

phonon interaction has been proposed[60] for the structure near 12200 cm^{-1}. The splittings of about 1800 cm^{-1} each would necessitate the generation of three LO phonons to explain the 12200 and 18800 cm^{-1} maxima as phonon side bands of their respective antecedent bands. If, however, the remarkable no-phonon-like peak at 9800 cm^{-1} is taken as the first transition energy, the 10400 cm^{-1} band becomes comprehensible in terms of one-phonon processes with LO$\simeq$600 cm^{-1}. A preliminary check of the excitation structures against the known level systems of $3d$ impurities reveals no simple relationship. Therefore West *et al.*[62] argue that charge transfer processes are represented by this excitation spectrum rather than internal transitions, a proposal which is not convincing in view of the outline of the spectrum.

The main points to be covered by a comprehensive model of the mechanisms of charge changes at copper centers concern the Cu^{2+} infrared absorption and the Cu green luminescence (cf., review[1]). Up to now, not even a unique model comprising both these phenomena has been accepted. A trial is made here to derive some of the main features of these optical transitions from an energy level scheme which is based on *e*- and *t*-type one-electron states of the impurities. The stronger the crystal field, the more this description should hold true. The diagrammatic representation of interconfigurational transitions has been used by various authors[76–78] for general arguments. Its validity is restricted to estimations of the overall properties of charge transfer and must not be extended to include finer details of the spectra.

All considerations start with and rest upon the statement of copper being incorporated as $[Cu^{2+}_{Zn}(d^9)]^{\times}$, a matter of fact which seems to be accepted indisputedly.[10] Therefore, Cu^{2+} is the central entity in the proposed scheme (Fig. 8). Its ambivalent capabilities are represented by the possibility of either donating electrons (to the left in Fig. 8) or holes (to the right). The internal

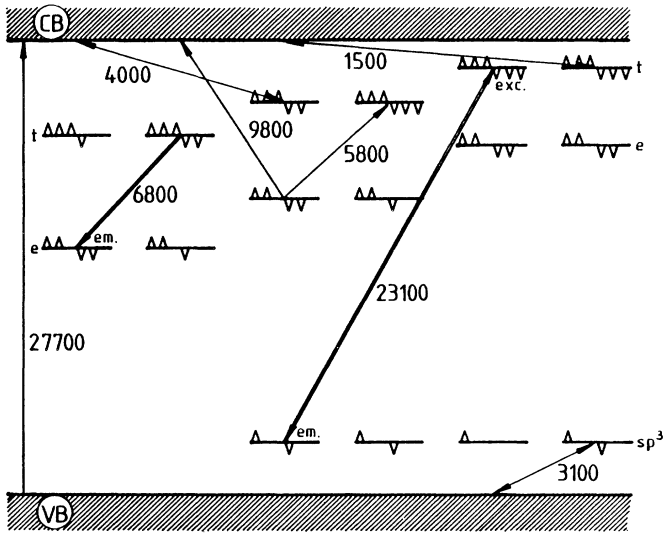

configuration	d^8	d^{8*}	d^9	d^{9*}	$d^{10}h^+$	d^{10}
strong-field quantum number	e^4t^4	e.g. e^3t^5	e^4t^5	e^3t^6	$e^4t^6h^+$	e^4t^6
spectroscopic symbol in T_d	$^3T_1$	e.g. $^3T_2$	$^2T_2$	^2E	$^2A_1$	$^1A_1$
effective charge	$D^\cdot$	$D^{\cdot *}$	$D^\times \equiv A^\times$	$A^{\times *}$	$[A{\cdot}X]^\times$	A'
ion charge	Cu^{3+}	Cu^{3+*}	Cu^{2+}	Cu^{2+*}	$Cu^{2+}{\cdot}X$	Cu^+

FIG. 8. Energy levels and transitions of the Cu ion in various charge states as represented by the corresponding one-electron configurations. The small pointers Λ and V indicate the occupancy of the levels by spin-up and spin-down electrons, respectively. Where (approximate) wave numbers $\bar{\nu}$ in cm^{-1} are given for the transition threshold energies, these have been drawn to scale. The configurations d^8 and d^{8*}, however, are not fixed with respect to the band edges. Electron notation throughout, i.e., transitions pointing upwards, are absorptions; downward arrows designate emissions. CB denotes conduction band, VB, valence bands, and X, exciton. An asterisk ($*$) labels excited states. (For d^{8*}, different excited states are possible, $^3T_2$ is but the lowest one.) Ionic charges are notated as 0, $+$, or $-$, whereas effective charge states are given as, $\times$, $\cdot$, or $'$.

$^2E(D) \leftarrow\!\!- {}^2T_2(D)$ absorption of d^9 is the lowest known excitation. In a higher excitation step, a hole is transferred from a d orbital to one of the binding orbitals of the surrounding oxygen ligands.[79] The reverse transition gives rise to the green luminescence of ZnO:Cu which exhibits a $\Gamma_4 \rightarrow \Gamma_4$ type ($\overline{C_{3v}}$) no-phonon line coinciding with the lowest-energy line α in the excitation spectrum.[80] The excited state of the Cu center which precedes the radiative recombination can be envisaged as a hole bound to the d^{10} closed shell or as an exciton X bound to the neutral d^9 configuration. An interpretation of the excitation fine structure and its Zeeman splitting is intelligible if properties of the valence bands are attributed to the hole states involved.[81] An energy of 3600 cm^{-1} is required[79] to eject the hole totally from the $Cu^{2+}X$ state. The value of 3100 cm^{-1} given in Fig. 8 is based on the measured depth of the A' acceptor level beneath the conduction band. While Dingle[79] postulates 800 cm^{-1} or less for this electron trapping energy, more recent measurements[82–85] yield 1400—1500 cm^{-1}. The position of the $Cu^+(d^{10})$ center is thus fixed in the band gap. The consecutive absorption processes $d^9 \rightarrow d^{10}h^+ \rightarrow d^{10}$ represent a two-step release of a hole from the Cu acceptor. The inverse step $d^{10} \rightarrow d^{10}h^+$, that is hole capture by Cu^+, could, on the other hand, render excitation of green emission possible, starting from a Cu^+ center (cf., Ref. 1 for details). Consequently, this step has been included in a model for the decay of the green luminescence.[86]

Detection of d^8 by EPR is not possible because of its Γ_1-A_1 ground state (cf., Fig. 6). Detection by optical absorption is, in general, a less sensitive method. Moreover, electron capture will lead to back-transformation $d^8 \rightarrow d^9$ with high efficiency, if any d^8 centers have been generated. Therefore, excitation of d^8 luminescence will most probably commence from the stable d^9 centers which are amply available in the crystal. Two processes are conceivable by which excited d^{8*} centers can be created,

$$Cu^{2+}(d^9) + e^{\cdot}_{VB} \rightarrow Cu^{3+}(d^{8*}) , \tag{5}$$

$$Cu^{2+}(d^9) + h\nu(d^9/d^{8*}) \rightarrow Cu^{3+}(d^{8*}) + e'_{CB} . \tag{6}$$

The first of these mechanisms would presume the existence of free holes. Although these are extremely short-lived in this n-type semiconductor, they could be generated according to

$$Cu^{2+}(d^9) + h\nu(d^9/d^{10}) \rightarrow Cu^{+}(d^{10}) + e^{\cdot}_{VB} . \tag{7}$$

This is also a sum reaction for the sequence of processes described earlier in this section. Together with (5), reaction (7) would constitute a disproportionation of $2Cu^{2+}$ into Cu^+ and Cu^{3+}. The energy involved in reaction (7) is about 26 200 cm^{-1}, as read from Fig. 8. Even if the

release of the hole is subdivided into consecutive steps, the highest step still requires about 23 100 cm^{-1} (or at least 17 300 cm^{-1}, if the hypothetical process $d^{9*} \rightarrow d^{10}h^+$ were effective) and this is the minimum energy necessary to produce the hole in a cascade process whose gross effect is given by (7). The excitation spectrum proves that these mechanisms are missing ($\bar{\nu} \gtrsim 23\,100$ cm^{-1}, cf. Ref. 60) or ineffective anyway (17 300 $cm^{-1} \lesssim \bar{\nu} \lesssim 22\,000$ cm^{-1}, cf., Fig. 7). Therefore, reaction (5) is abandoned for it could only contribute to a minor extent to the d^{8*} excitation, i.e., only as far as shallow hole traps[86,87] may provide the required holes.

Reaction (6) is thus left as the probable source for excited d^{8*} centers. The model of Fig. 8 is unsuitable to predict a minimum energy for this ionization of d^9 unless supplemented by experimental evidence. A rough estimate based on the d^9/d^{10} levels yields $(5800 + 1500)$ $cm^{-1} = 7300$ cm^{-1} with complete neglect of the expected level shift due to the change of the charge state. Since the mechanism (6) will work as well with photon energies above this conjectural threshold, an excitation spectrum is expected which bears some of the structure of the d^8 excited states. These can be determined by one of the known multiplet treatments.[88-90] The recording of such structures is enabled by the fact that the competing acceptor-type absorption processes do not set in before $\bar{\nu} \gtrsim 23\,000$ cm^{-1}. It is thus a straightforward consequence of the proposed model that the excitation of this $Cu^{3+}(d^8)$, i.e., "donor-type" emission would cease as soon as the energy is sufficient to provoke "acceptor-type" transitions (cf., Fig. 7). An assignment of the excitation structures to particular transitions, e.g., in a Tanabe-Sugano diagram[88] necessitates the determination of the amount of energy in (5) which is consumed to liberate the carrier e'_{CB}. A simple subtraction of the rough 7300-cm^{-1} threshold from the energies read from Fig. 7 leads to unplausible low energies for the d^{8*} levels. Therefore, a deductive way will be followed to harmonize the excitation structures with estimates based on crystal-field empiricism.

In the static crystal-field approximation,[16] the cubic spin-orbit component T_1-$^3T_1(F)$ (cf., Fig. 6) is placed by $\frac{3}{2}|\lambda_c|$ above the d^8 ground state. The weighed mean of the present Γ_3 and Γ_2 components yields 582 cm^{-1} for this elevation, thus the spin-orbit coupling parameter $|\lambda_c| = 388$ cm^{-1}. The main emission line E_I with the wave number $\bar{\nu}_I$ then renders by $\bar{\nu}_I = 8Dq + 2.5|\lambda_c|$ the cubic-crystal-field parameter $Dq \simeq 740$ cm^{-1}. For a free Cu^{3+} ion, the Racah parameter B_0 can be expected in the interval 1174 cm^{-1} (Ref. 91) $\lesssim B_0 \lesssim$ 1400 cm^{-1} (Ref. 92). The solid-state reduction of the electron repulsion is evaluated by Phillips's ionicity[93] which is $f_i = 0.62$ for ZnO, hence $B \simeq 800$ cm^{-1} will be assumed. Extrapolations yield a mean value of 4.4 for the ratio C/B (after Refs. 91, 92, and 94), so that the electron interaction parameter $C \simeq 3500$ cm^{-1}. The quantities derived are needed to read a set of "predicted" transition energies from a Tanabe-Sugano[88] diagram for a d^8 ion in tetrahedral coordination. With somewhat increased accuracy this can also be accomplished with the help of Ref. 95. Utilization of these plots requires the knowledge of Dq, B, and C. With $B = 860$ cm^{-1} and $C/B = 4.4$ (Ref. 88) or $B = 810$ cm^{-1} and $C/B = 3.9$ (Ref. 95), the published diagrams[88,95] provide enough fidelity to justify their direct application for the present purpose.

If the plots are entered with $Dq = 740$ cm^{-1}, the experimental threshold energies in the excitation spectrum bear but little resemblance to the set of intersection points, except for the first excited state $^3T_2(F)$. The empirical values should, however, be corrected by subtraction of a $d^9 \rightarrow d^{8*}$ photoionization energy $\bar{\nu}(d^9/d^{8*})$, cf., reaction (6). Naturally, the emitting $^3T_2(F)$ state now has to be exempted from the desired fit. A crude approximation of the experimental values is possible with $\nu(d^9/d^{8*}) \simeq 4000$ cm^{-1}. The fit can be improved in the Liehr-Ballhausen plot[95] by shifting to a diminished $Dq \simeq 650$ cm^{-1}, where a $\bar{\nu}(d^9/d^{8*}) \simeq 3800$ cm^{-1} results. The numerical conformity is remarkable but still limited by inherent errors both in the derviation of the experimental values from Fig. 7 and in the application of the plots[88,95] involving only approximate parameters. The numbers (Table I) are valid for the medium crystal-field case and infer that all of the occur-

TABLE I. Interpretation of the ZnO:Cu excitation spectrum (Fig. 7) in terms of $Cu^{2+}(d^9) \rightarrow Cu^{3+}(d^{8*})$ transitions.

Assignment (upper level)	Transition energy uncorrected[a] cm^{-1}	Transition energy fitted[b] cm^{-1}	Experimental value (read from Fig. 7) threshold energy cm^{-1}	Experimental value (read from Fig. 7) band maximum cm^{-1}	Remarks
$T_2 - {}^3T_2(F)$	6 100	9 900	9 800	10 400	combined spin-orbit and C_{3v} splittings
$\Gamma_3 - E - {}^3T_2(F)$	6 700	10 500	11 400	12 100	
$^1T_2(D)$	11 500	15 300	15 600	17 100	c
$^1E(D)$	12 700	16 500	17 000	18 700	
$T_2 - {}^3A_2(F)$	13 200	17 000	not observed		c,d
$T_2 - {}^3T_1(P)$	17 200	21 000	present as an unresolved structure		

[a]As read from Ref. 95 at $Dq = 650$ cm^{-1}.

[b]Corrected by adding a photoionization energy assumed as $\bar{\nu}(d^9/d^{8*}) = 3800$ cm^{-1}, see text.

[c]Mixing of T_2 levels of different origin.

[d]The transition to this e^2t^6 configuration is strongly forbidden from the e^4t^5 ground state (except for possible mixing effects).

ring absorption transitions are allowed. The relative strengths of the observed excitation bands and their widths are in plausible concordance with the expectations from this assignment.

In the respective Dq region, a mixing of T_2 components of the ^1D and the ^3F terms appears and a noncrossing rule holds for the levels labeled by the same irreps. Nevertheless, the singlet levels are evidently taking part in the excitation processes. Spectroscopy with ZnS:Ni^{2+} has also proved[96] the participation of d^8 singlets in the excitation of luminescence. The d^8 levels above T_2-$^3T_1(P)$ are not suitable for excitation because of the competing acceptor-type optical processes mentioned. The splitting of the dominating excitation bands in the (10 000—13 000)-cm^{-1} region (cf., Fig. 7) is now related to the spin-orbit splitting[16,36,97] of the $^3T_2(F)$ level (cf., Fig. 6). From the A_1 ground state in a T_d environment, only the absorption terminating in T_2-$^3T_2(F)$ is allowed whereas by lowering the symmetry to C_{3v}, transitions to Γ_3-E-$^3T_2(F)$ become allowed additionally ($\mathbf{E}\perp\mathbf{c}$). Thus, the two main bands of this transition find an unconstrained interpretation. The order of magnitude estimated for the overall spin-orbit splitting[16,36,97] of $^3T_2(F)$ conforms with the observed splitting. A numerical interpretation would require a spin-polarized version of the model, but, for the first time a general explanation of the excitation structure is offered, based on a d^9 photoionization with concurrent d^8 internal absorptions involving an approximate $Dq\simeq 700$ cm^{-1}.

With the parameter $\lambda_c=-388$ cm^{-1} being fixed for the ground term multiplet, the T_2,E-$^3T_1(F)$ spin-orbit components (cf., Fig. 6) can be predicted at $4.5\,|\lambda|\simeq 1750$ cm^{-1} (according to Ref. 16). One of the ZnO crystals used here displays a structured absorption at low temperatures in the $(1400\lesssim\nu\lesssim 1600)$-$cm^{-1}$ spectral range different from the threshold-type behavior expected for the $d^{10}\rightarrow d^9$ transition which is anticipated in this same spectral region. Although a more thorough investigation of this effect is intended, it can tentatively be attributed to transitions terminating in these levels.

Inspection of Fig. 8 shows that two different thresholds follow for $d^8\rightleftarrows d^9$ conversions. The energy of 9800 cm^{-1} for the excitation of the T_2-$^3T_2(F)$ level of d^8 (cf., Fig. 7) implies a photoionization energy of roughly $\bar{\nu}\simeq 3800$ cm^{-1} (cf., Table I). Nearly the same energy results by subtraction of the d^9 internal transition energy 5800 cm^{-1} from the 9800 cm^{-1} threshold. Consequently, if the d^8 ground state e^4t^4 is involved in the $d^8\rightleftarrows d^9$ conversion (instead of one of the excited states, e.g., e^3t^5), a transition energy 4000 cm^{-1} is predicted. In this energy range, distinct structures are recorded[85] for the photoionization cross section of an unidentified "deep donor" in ZnO:Cu.

Finally, the model has important consequences for the absence[59,60,62] of the internal $^2E\rightarrow{}^2T_2$ transition of Cu^{2+} in the emission spectrum of ZnO:Cu. This is in contrast to ZnS:Cu where the Cu levels are located much lower in the band gap.[98,99] Since the attempts to excite this emission have been carried out under irradiation with visible light, $d^9\rightarrow d^{8*}$ processes are initiated. The competing d^8 emission can only be excluded by excitation with $\bar{\nu}\lesssim 9000$ cm^{-1}. Regarding the corresponding d^9 absorption spectrum,[35,58,59] excitation can only be expected with any appreciable efficiency in the very limited range 5900 $cm^{-1}\lesssim\bar{\nu}\lesssim$ 6800 cm^{-1}. And even then a two-step excitation $d^9\rightarrow d^{9*}\rightarrow d^{8*}$ is conceivable which would again infer d^8 emission. The present model thus contains, for the first time, a solution to the problem of the missing d^9 emission. There are still simplifications involved, of course, among which are neglect of spin, of interplay with other centers, e.g., imperfections, of donor-acceptor interaction, of nonradiative processes, and of covalency. But although the model is not in all details backed by conclusive evidence, it is intended as an aid for future investigations.

VII. DISCUSSION

A. Chemical trends in crystal field parameters

A comparison seems appropriate which relates the internal and the charge exchange transitions of $Ni^{3+}(d^7)$ and $Cu^{3+}(d^8)$ with those of other $3d$ ions in ZnO or of the same centers in different host materials. The parameters are tabulated which have been derived for the isoelectronic ions Co^{2+} and Ni^{2+} and are confronted with approximate figures inferred from the present data for Ni^{3+} and Cu^{3+}. However, features which are inherent to the particular model applied influence the resulting numbers. Among these interactions are various electron-electron effects, including spin-related effects, and electron-phonon coupling. Several proposals have been presented[89,100,101] which indicate various ways to allow for some of these effects. Implications of the models to explain or predict chemical trends in the sequence of $3d$ elements or among corresponding centers in a series of lattices have been studied.[71,89,102–106] With only a few exceptions,[71,89] neither ZnO nor the triply positive transition ions are treated in these trend studies. To evaluate the present results, some of the published material shall be quoted (Tables II and III). The principal ways of doing this include comparison with (i) free-ion data, (ii) properties of the same ion in other comparable host materials, (iii) isoelectronic ions in ZnO, (iv) different states of ionization of the same dopant.

The emission of Ni^{3+} involves the low-lying energy levels of d^7 only whose splitting does not allow direct conclusions on the parameters B or C. Reduction by f_i, of the free-ion value B_0 which can be extrapolated as 1150 $cm^{-1}\lesssim B_0\lesssim 1500$ cm^{-1} (after Figgis[92]) yields $B\simeq 820$ cm^{-1}. Various sources[92,94] give $\lambda_0\simeq 235$ cm^{-1} which leads to $f_i\lambda_0\simeq 146$ cm^{-1}, in nice agreement with the most reliable experimental value[18] for ZnO:Co^{2+} (cf., Table II). The relation $2D=\lambda_e(g_{\|}-g_{\perp})$ with the difference $g_{\|}-g_{\perp}=-0.016\,35$ of Ref. 44 and our experimental value $2D=5.7$ cm^{-1} entail a $\lambda_e\simeq 350$ cm^{-1} which even exceeds the free-ion value λ_0. The absence[18] of Jahn-Teller interaction at ZnO:Co^{2+} leads to the same expectation for ZnO:Ni^{3+} here and would therefore exclude a quenching of λ by dynamic effects. The deviation could, however, be due to a flaw in the g anisotropy. The cubic-crystal-field parameter Dq is determined by the transition energy. If allowance is made for the trigonal field and spin-orbit effects, $Dq\simeq 630$ cm^{-1} is estimated. This is

TABLE II. Comparison of the d^7 ions Co^{2+} and Ni^{3+} in various environments.

Quantity (unit) \ Material	Free Co^{2+} ion	$ZnO:Co^{2+}$			Free Ni^{3+} ion	$ZnS:Ni^{3+}$	$ZnO:Ni^{3+}$	
Source	Figgis[a]	Weakliem[b]	Jugessur[c] *et al.*	Koidl[d]	McClure[e]	Holton *et al.*[f]	Holton *et al.*[f]	Present paper
Dq (cm^{-1})		390	406	400			(>400)	630
$2D$ (cm^{-1})		≃1	0.7	5.4			4	5.7
B (cm^{-1})	1120	775	770	760	1115			(820)
C (cm^{-1})	4370	3490		3500	5450			
C/B	3.9	4.5		4.6	4.9			
$\lvert\lambda\rvert$ (cm^{-1})	172	210	172	143	235[a]		(<238)	(350)[h]
$g_{\parallel}$			2.105	(2.22)		2.148	2.143	
$g_{\perp}$			2.101	(2.26)		(isotropic with cubic ZnS)	4.318[g]	
Remarks		absorption at $T=77$ K	MO theory	absorption at $T=4.2$ K		EPR at $T\simeq1.3$ K	EPR at $1K\lesssim T\lesssim4$ K	emission $T\simeq4$ K

[a]Reference 92.
[b]Reference 16.
[c]Reference 107.
[d]Reference 18.
[e]Reference 91.
[f]Reference 44.
[g]With effective spin $S'=\frac{1}{2}$ (confirmed by Hausmann, Ref. 34 for $ZnO:Co^{2+}$). With $S=\frac{3}{2}$, $g_{\parallel}$ would not change but $g_{\perp}$ would be half the value given, i.e.,) $g\simeq2.159$.
[h]Based on the g anisotropy of Holton *et al.*, Ref. 44, and a spin Hamiltonian with $S=\frac{3}{2}$.

TABLE III. Comparison of the d^8 ions Ni^{2+} and Cu^{3+} in various environments.

Quantity (unit) \ Material	Free Ni^{2+} ion	$ZnS:Ni^{2+}$			$ZnO:Ni^{2+}$			Free Cu^{3+} ion	$ZnS:Cu^{3+}$	$ZnO:Cu^{3+}$
Source	Figgis[a]	Weakliem[b]	Kaufmann *et al.*[c]	Roussos and Schulz[d]	Weakliem[b]	Kaufmann *et al.*[c]	Brumage and Lin[e]	McClure[f] and Figgis[a]	Herrig *et al.*[g]	Present paper
Dq (cm^{-1})		475	413		420	411				700[k]
$\bar{\nu}(T_1)$-$\bar{\nu}(A_1)$ for $^3T_1(F)$		(340)		179	(340)[j]		227[j]		(270)	582
B (cm^{-1})	1080	560	592		770	777		1280		800
C (cm^{-1})	4860	2520	2215		3700	3420		5630		3520
C/B	4.5	4.5	3.7		4.8	4.4		4.4		4.4
$\lvert\lambda\rvert$ (cm^{-1})	315	(250)	(250)[h]	120[i]	(250)[j]	(250)[h]	175	445	178	388[i]
Remarks		absorption at $T=77$ K	absorption at $T=6$ K	emission at $T\simeq2$ K	absorption at $T=77$ K	absorption at $T=6$ K	magnetic susceptibility	extrapolations	absorption of Cu associates at $T\simeq5$ K	photoluminescence at $T\simeq4$ K

[a]Reference 92.
[b]Reference 16.
[c]Reference 36.
[d]Reference 29.
[e]Reference 67.
[f]Reference 91.
[g]Reference 65.
[h]Static crystal field model considered as inadequate, since a dynamic Jahn-Teller effect is acting on $^3T_2(F)$.
[i]Static crystal field model according to Weakliem, Ref. 16.
[j]The weighted mean value 220 cm^{-1} (Anderson, Ref. 17) implies $\lvert\lambda\rvert\simeq150$ cm^{-1}.
[k]Averaged from 740 cm^{-1} (emission) and 650 cm^{-1} (excitation spectrum).

strongly increased versus the Ni^{2+} ion in ZnO (cf. Table III) with $Dq=411$ cm^{-1} (Ref. 36) or the isoelectronic Co^{2+} ion (Table II) for which $Dq\simeq 400$ cm^{-1} in ZnO (Ref. 18). This is in concord with the general observations of a rise in Dq (i) on progressing ionization of the same ion[91] or (ii) with an increase of the nuclear charge of the central ion.[44] Both effects are related to the decreasing effective bond length.

For the $Cu^{3+}(d^8)$ ion, some of the ZnO crystal field parameters have been derived and discussed in Sec. VI C (cf. Table III). Optical transitions within a Cu^{3+} ion have been quoted[65] for an associated center $[Cu^{3+}, Y]$ in ZnS involving an unknown partner Y. Even earlier[108] had the participation of Cu^{3+} been postulated in a complex "Cu-R" which gives rise to a photosensitive EPR signal in ZnS. The Dq value being unknown for ZnS:Cu^{3+}, only ZnO:Ni^{2+} is suited for comparison. Again, a pronounced increase in Dq is noticed for these d^8 configurations on increasing the charge of the central ion, i.e., on turning from Ni to Cu. Moreover, the rise of Dq is obvious, if the oxidation state is raised from Cu^{2+} to Cu^{3+} (cf. Fig. 8). Evidently, as the ligands are pulled in closer by the central ion, Dq grows from about 580 cm^{-1} for ZnO:Cu^{2+} (Ref. 58) to around 700 cm^{-1}, here. The increase of the effective spin-orbit parameter of ZnO:Cu^{3+}, $\lambda_c\simeq 0.87\ \lambda_0$ estimated here as compared to the value[36] of $\lambda\simeq 250$ cm^{-1} for Ni^{2+} is in reasonable agreement with expectations considering the increased free-ion parameter for this coupling in Cu^{3+} versus Ni^{2+} (cf., Table III).

B. Chemical trends in energies of charge transfer

The only theoretical approach to the problem of donor and acceptor energies in ZnO doped by $3d$ impurities is a recent cluster calculation.[71] The charge transfer transitions are estimated by the transition state method. The value obtained for the $d^9\rightarrow d^{10}$ acceptorlike transition of ZnO:Cu is lower than the experimental figure for $d^9\rightarrow d^{10}h^+$ by about 18%. The t_2-e distance of 6000 cm^{-1} obtained for Cu^{2+} is reasonable, for Cu^+ it is calculated to shrink to about 4000 cm^{-1}, the levels shifting upwards. While the trends in these results are in an overall agreement with the present semiempirical model, quantitative conclusions and consequences regarding the stability of different oxidation states should be considered with great care.

For Cu in ZnS, acceptor- and donor-type transitions are predicted by a semiempirical tight-binding scheme.[105] For ZnO:Ni, the donor-type transition, i.e., $d^8\rightarrow d^7$, should require about the same relative energy as $d^9\rightarrow d^8$ for ZnS:Cu, viz., about 22 400 cm^{-1} corrected for ZnO. This number is in concord with the threshold estimated from photo-stimulated Ni^{3+} EPR signals[44] and with that of Ref. 37, cf., Sec. IV. The actual mechanism of the $d^8\rightarrow d^7$ transformation is liable to a more complicated scheme [cf. reactions 4(a)—4(c)].

C. Aspects of vibronic processes

Three of the four emission bands presented in this study display satellites of the no-phonon lines due to impurity-lattice interactions. Some of the more prominent transitions in each of these luminescence spectra are listed in Table IV along with some of the phonons related to critical points of the Brillouin zone. As there exist deviating interpretations of ZnO phonon energies, a harmonized set of values is proposed here. The numbers

TABLE IV. Some of the more prominent phonon statellites identified in the emission spectra, compared with ZnO bulk phonons. The numbers in columns 3 to 5 are usually read from the figures with an accuracy of about ±5 cm^{-1}. In the first column, parentheses denote critical points of the Brillouin zone and square brackets indicate the symmetry of vibrational modes.

Assignment / Material	ZnO host lattice	ZnO:Co^{2+} d^7 $^4T_1(P),^2T_1(G),^2E(G)\rightarrow{}^4A_2(F)$	ZnO:Ni^{3+} d^7 $^4T_2(F)\rightarrow{}^4A_2(F)$	ZnO:Cu^{3+} d^8 $^3T_2(F)\rightarrow{}^3T_1(F)$
TA(A),TO(A)	75[a]			
TO(Γ)[E_2]	101[b]	105	105	100
LO(Γ)[B_1]	138[a]	135		140
LA(A),LO(A)	180[b]	185		
TO(Γ),LO(Γ)[c]	243[d]	250	250	270
TO(Γ)[A_1]	378[b]			
TO(Γ)[E_1]	410[b]		≃410	393
TO(A)	425[a]			
TO(Γ)[E_2]	440[b]	≃440		
LO(Γ)[c]	489[d]		500	500
LO(A)[c]	540[e]			540
LO(Γ)[A_1]	576[b]			
LO(Γ)[E_1]	587[b]	≃580	588	
		Fig. 2	Fig. 3	Fig. 5

[a]W. Wegener, Ref. 109.

[b]Averaged after Ref. 8.

[c]Reinterpretation of published data, based on Fig. 20 of Ref. 8 (after Ref. 49).

[d]S. S. Mitra, R. Marshall, Ref. 110.

[e]S. S. Mitra and J. I. Bryant; Ref. 68, J. M. Calleja and M. Cardona; Ref. 52. An interpretation of this mode as a combination according to 540 cm$^{-1}\simeq$(440 + 101) cm^{-1} is also conceivable.

have been obtained by averaging those compiled by Mollwo,[8] unless indicated otherwise. Where the assignments depart from those in the original papers, they are based on the phonon dispersion diagram.[49]

Except for TO(Γ), the impurity emissions are found to couple with essentially differing vibrational modes. This finding points towards the differing selection rules applicable to transitions between levels of different spectroscopic character. The numerical values derived from luminescence are, on the other hand, in satisfactory agreement with the listed ZnO bulk phonons. No "reduced" phonons which would indicate dynamic Jahn-Teller interaction, are recognized for the three bands considered. In the feeble Co^{2+} spectrum of Fig. 1, phonon-assisted transitions could not at all be discerned. The Ni^{3+} transition is coupled to E_1-type optical modes (active for $\mathbf{E}\perp\mathbf{c}$) rather than A_1. The other two bands display coupling to the mean values of A_1 and E_1 modes. A small broad peak near 22 805 cm^{-1} has recently been detected[111] in the green ZnO:Cu emission band. Its low-energy shift of about 265-cm^{-1} versus the main line α (cf., Ref. 80) is repeated several times in the positions of additional weak satellites. According to Table IV, this observation could be related to TO(Γ)/LO(Γ) phonon interaction.

VIII. CONCLUSIONS

New emission bands are detected with ZnO:Co crystals at $T\simeq 4$ K. By comparison with the coinciding no-phonon lines in absorption, a polarized doublet at $\bar{\nu}=3616$ ($\mathbf{E}\perp\mathbf{c}$); 3611 ($\mathbf{E}\|\mathbf{c}$) cm^{-1} (Fig. 1) is identified as the Γ_1-$^4T_2(F)\rightarrow\Gamma_2$-$^4A_2(F)$ transition of Co^{2+}_{Zn} ion in C_{3v} symmetry, the line separation of 5.7 cm^{-1} representing the spin-orbit splitting into Γ_5,Γ_6 and Γ_4 in the ground state. Another doublet at 15136;15132 cm^{-1} ($\mathbf{E}\perp\mathbf{c}$) (Fig. 2) is identified as a $^4T_1(P),^2T_1(G),^2E(G)\rightarrow{}^4A_2(F)$ transition.

With ZnO:Ni, an emission doublet at 6096;6090 cm^{-1} is resolved (Fig. 3) which corresponds to broad structures earlier observed at 90 K and attributed to Ni^{2+}. The transition energy does not, however, comply with the Ni^{2+} levels derived from absorption spectra. The emission exhibits several similarities with the Co^{2+} spectrum regarding fine structure, polarization, and thermalization. These now lead to an interpretation in terms of the corresponding $^4T_2(F)\rightarrow{}^4A_2(F)$ internal transition of $Ni^{3+}(d^7)$. The light-stimulated generation of Ni^{3+} is discussed which has been proved earlier by EPR. While the direct $d^8\rightarrow d^7$ conversion is a forbidden process under electric-dipole selection rules, a sequence of processes is proposed which generates an excited state of the d^7 configuration commencing from the stable $Ni^{2+}(d^8)$ ground state whose presence is proved by absorption spectroscopy (Fig. 4).

The polarization properties of the infrared emission of ZnO:Cu have been studied at $T\simeq 4.2$ K (Fig. 5). An interpretation is suggested by the details in the fine-structure which relates the three main lines E_{I}–E_{III} at 6887, 6374, and 6270 cm^{-1} with Γ_1-T_2-$^3T_2(F)\rightarrow\Gamma_1$-$A_1$-$^3T_1(F)$ and $\rightarrow\Gamma_2,\Gamma_3$-$T_1$-$^3T_1(F)$ transitions, respectively, in a $3d^8$ configuration of Cu^{3+} (Fig. 6). These internal $3d^8$ radiative transitions become explicable in a model of one-electron configurations (Fig. 8) comprising $d^9\rightarrow d^{8*}$ charge transfer transitions. Excitation spectroscopy of this photoluminescence (Fig. 7) promotes an assignment of the main bands (Table I) as absorption transitions from the $Cu^{2+}(d^9)$ ground state into various excited states of $Cu^{3+}(d^8)$.

This is probably the first example where a sequence of excited states becomes accessible for a transient charge state of an impurity in a semiconductor. The optical excitation processes commencing from one of its stable configurations imply the feasibility of emission processes in a particular charge state of this defect without necessitating its long-term stability. The discussion of the parameters derived from the experiments and the suggested interpretations yield a reasonable concord with quoted crystal-field (Tables II and III) and phonon data (Table IV).[112]

ACKNOWLEDGMENTS

This work was carried out with crystal material grown by Professor Dr. R. Helbig and his collaborators in the Institut für Angewandte Physik der Universität Erlangen-Nürnberg. Supporting EPR and IR spectra were taken by Dr. J. Nagel, a microprobe analysis was taken by Dr. K. Müller and Frau G. Weinberg. We would like to express our gratitude to all of them.

[1]H.-J. Schulz, in *Zinc Oxide,* Vol. 7 of *Current Topics in Materials Science* edited by E. Kaldis (North-Holland, Amsterdam, 1981), p. 241.

[2]U. Rössler, Phys. Rev. **184**, 733 (1969).

[3]S. Bloom and J. Ortenburger, Phys. Status Solidi B **58**, 561 (1973).

[4]J. R. Chelikowsky, Solid State Commun. **22**, 351 (1977).

[5]A. Kobayashi, O. F. Sankey, and J. D. Dow, Phys. Rev. B **28**, 946 (1983).

[6]H. E. Brown, *Zinc oxide: Properties and Applications* (Intl. Lead Zinc Research Organization, New York, 1976).

[7]W. Hirschwald, P. Bonasewicz, L. Ernst, M. Grade, D. Hofmann, S. Krebs, R. Littbarski, G. Neumann, M. Grunze, D. Kolb, and H.-J. Schulz, in *Zinc Oxide,* Vol. 7 of *Current Topics in Materials Science,* Ref. 1, p. 143.

[8]E. Mollwo, *Physics of II-VI and I-VII Compounds, Semimagnetic Semiconductors,* Vol. 17b of *Landolt-Börnstein,* (Springer-Verlag, Berlin, 1982), pp. 35 and 335.

[9]D. M. Kolb, in *Zinc Oxide,* Vol. 7 of *Current Topics in Materials Science,* Ref. 1, p. 226.

[10]G. Müller and R. Helbig, J. Phys. Chem. Solids **32**, 1971 (1971).

[11]R. Helbig, J. Cryst. Growth **15**, 25 (1972).

[12]F. W. Kleinlein and R. Helbig, Z. Phys. **266**, 201 (1974).

[13]W. Feitknecht, Helv. Chim. Acta **20**, 659 (1937).

[14]D. S. McClure, J. Phys. Chem. Solids **3**, 311 (1957).

[15]R. Pappalardo, D. L. Wood, and R. C. Linares, J. Chem. Phys. **35**, 2041 (1961).

[16]H. A. Weakliem, J. Chem. Phys. **36**, 2117 (1962).

[17]R. S. Anderson, Phys. Rev. **164**, 398 (1967).

[18]P. Koidl, Phys. Rev. B **15**, 2493 (1977).

[19]E. Ziegler, A. Heinrich, H. Oppermann, and G. Stover, Phys. Status Solidi A **70**, 563 (1982).

[20]T. L. Estle and M. De Wit, Bull. Am. Phys. Soc. **6**, 445 (1961).

[21]In concord with widespread usage, the transitions are measured in wave numbers $\bar{\nu}=\lambda^{-1}$ throughout. These values, given in cm^{-1}, are sometimes called "energies" although correctly $E=h\nu=hc\bar{\nu}$.

[22]The notation of Koster *et al.* 1963 is used in this paper for the irreducible representations of C_{3v} and the related double group $\overline{C_{3v}}$; G. F. Koster, J. O. Dimmock, R. G. Wheeler, and H. Statz, *Properties of the Thirty-Two Point Groups* (M.I.T. Press, Cambridge, 1963).

[23]G. Roussos, J. Nagel, and H.-J. Schulz, Z. Phys. B **53**, 95 (1983).

[24]U. G. Kaufmann and P. Koidl, J. Phys. C **7**, 791 (1974).

[25]I. Broser, R. Germer, and H.-J. Schulz, J. Magn. Magn. Mater. **15-18**, 29 (1980).

[26]B. Nestler and U. Scherz, J. Lumin. **24-25**, 229 (1981).

[27]D. Buhmann, H.-J. Schulz, and M. Thiede, Phys. Rev. B **19**, 5360 (1979).

[28]D. J. Robbins, P. J. Dean, J. L. Glasper, and S. G. Bishop, Solid State Commun. **36**, 61 (1980).

[29]G. Roussos and H.-J. Schulz, Phys. Status Solidi B, **100**, 577 (1980).

[30]G. Roussos and H.-J. Schulz, Solid State Commun. **51**, 663 (1984).

[31]D. Buhmann, H.-J. Schulz, and M. Thiede, Phys. Rev. B **24**, 6221 (1981).

[32]Y. Kanai, J. Phys. Soc. Jpn. **24**, 956 (1968).

[33]D. Fichou, Ph. D. thesis, Université Pierre et Marie Curie, Paris, 1986.

[34]A. Hausmann, Phys. Status Solidi **31**, K131 (1969).

[35]R. Pappalardo, D. L. Wood, and R. C. Linares, J. Chem. Phys. **35**, 1460 (1961).

[36]U. Kaufmann, P. Koidl, and O. F. Schirmer, J. Phys. C **6**, 310 (1973).

[37]M. L. Reynolds and G. F. J. Garlick, Infrared Phys. **7**, 151 (1967).

[38]M. L. Reynolds, W. E. Hagston, and G. F. J. Garlick, Phys. Status Solidi **33**, 579 (1969).

[39]S. G. Bishop, P. J. Dean, P. Porteous, and D. J. Robbins, J. Phys. C **13**, 1331 (1980).

[40]A. Karipidou, H. Nelkowski, and G. Roussos, J. Cryst. Growth **59**, 307 (1982).

[41]G. Goetz, G. Roussos, and H.-J. Schulz, Solid State Commun. **57**, 343 (1986).

[42]B. Clerjaud, A. Gelineau, F. Gendron, C. Porte, J. M. Baranowski, and Z. Liro, Physica B + C, **116**, 500 (1983).

[43]W. Busse, H.-E. Gumlich, D. Maier-Hosch, E. Neumann, and H.-J. Schulz, J. Lumin. **1/2**, 66 (1970).

[44]W. C. Holton, J. Schneider, and T. L. Estle, Phys. Rev. **133**, A1638 (1964).

[45]M. De Wit, T. L. Estle, W. C. Holton, and J. Schneider, Bull. Am. Phys. Soc. **9**, 249 (1964).

[46]M. Schulz, Ph.D. thesis, Technische Universität Berlin, 1971.

[47]T. C. Damen, S.P.S. Porto, and B. Tell, Phys. Rev. **142**, 570 (1966).

[48]C. A. Arguello, D. L. Rousseau, and S. P. S. Porto, Phys. Rev. **181**, 1351 (1969).

[49]A. W. Hewat, Solid State Commun. **8**, 187 (1970).

[50]W. Wegner and S. Hautecler, Phys. Lett. **31A**, 2 (1970).

[51]K. Thoma, B. Dorner, G. Duesing, and W. Wegener, Solid State Commun. **15**, 1111 (1974).

[52]J. M. Calleja and M. Cardona, Phys. Rev. B **16**, 3753 (1977).

[53]G. F. J. Garlick, *Licht und Materie*, Vol. 26 of *Handbuch der Physik*, edited by S. Flügge (Springer-Verlag, Berlin, 1958), p. 29.

[54]I. Broser, K.-H. Franke, M. G. Gafron, R. T. Heinze, H. Maier, U. Scherz, H.-J. Schulz, M. Schulz, and M. Wöhlecke, Verhandlungen DPG [VI] **4**, 156 (1969).

[55]R. Pappalardo, J. Molecular Spectrosc. **6**, 554 (1961).

[56]R. Pappalardo and R. E. Dietz, Phys. Rev. **123**, 1188 (1961).

[57]H. A Weakliem and D. S. McClure, J. Appl. Phys. **33**, 347 (1962).

[58]R. E. Dietz, H. Kamimura, M. D. Sturge, and A. Yariv, Phys. Rev. **132**, 1559 (1963).

[59]R. Heinze, Ph.D. thesis, Technische Universität Berlin, 1975.

[60]P. J. Dean, D. J. Robbins, S. G. Bishop, J. A. Savage, and P. Porteous, J. Phys. C **14**, 2847 (1981).

[61]D. Zwingel, Phys. Status Solidi B **67**, 507 (1975).

[62]C. West, D. J. Robbins, P. J. Dean, and W. Hayes, Physica B + C, **116**, 492 (1983).

[63]I. Broser and M. Schulz, Solid State Commun. **7**, 651 (1969).

[64]A. Hausmann, B. Schallenberger, and R. Roll, Z. Phys. B **34**, 129 (1979).

[65]L. Herrig, J. Nagel, and H.-J. Schulz, J. Phys. (Paris) **44**, 1317 (1983).

[66]G. Roussos and H.-J. Schulz, J. Lumin. **31/32**, 427 (1984).

[67]W. H. Brumage and C. C. Lin, Phys. Rev. **134**, A950 (1964).

[68]S. S. Mitra and J. I. Bryant, Bull. Am. Phys. Soc. (2) **10**, 333 (1965).

[69]U. Kaufmann and O. F. Schirmer, Optics Commun. **4**, 234 (1971).

[70]M. Sumita, Jpn. J. Appl. Phys. **6**, 1469 (1967).

[71]N. Gemma, J. Phys. C **17**, 2333 (1984).

[72]G. Roussos (private communication).

[73]J. W. Allen, J. Phys. C **2**, 1077 (1969).

[74]J. M. Langer, Phys. Status Solidi B **47**, 443 (1971).

[75]K. A. Kikoin and V. N. Fleurov, Solid State Commun. **39**, 1281 (1981).

[76]J. M. Noras and J. W. Allen, J. Phys. C **13**, 3511 (1980).

[77]V. N. Fleurov and K. A. Kikoin, Solid State Commun. **42**, 353 (1982).

[78]V. F. Masterov, Fiz. Tekh. Poluprovodn. **18**, 3 (1984); [Sov. Phys.—Semicond. **18**, 1 (1984)].

[79]R. Dingle, Phys. Rev. Lett. **23**, 579 (1969).

[80]I. Broser, R. Germer, H.-J. Schulz, and K. Wisznewski, Solid State Electron. **21**, 1597 (1978).

[81]D. J. Robbins, D. C. Herbert, and P. J. Dean, J. Phys. C **14**, 2859 (1981).

[82]E. Mollwo, G. Müller, and P. Wagner, Solid State Commun. **13**, 1283 (1973).

[83]G. Müller, Phys. Status Solidi B **76**, 525 (1976).

[84]H. G. Grimmeiss, J. Crystal Growth **59**, 40 (1982).

[85]N. Kullendorff and R. Helbig, paper included in thesis of N. Kullendorff, University of Lund, Sweden, 1982.

[86]R. Kammermayer, V. Wittwer, N. Eisenreich, and K. Luchner, Solid State Commun. **19**, 461 (1976).

[87]V. Wittwer and K. Luchner, Phys. Status Solidi A **25**, 559 (1974).

[88]Y. Tanabe and S. Sugano, J. Phys. Soc. Jpn. **9**, 753 (1954) & **9**, 766 (1954).

[89]A. Fazzio, M. J. Caldas, and A. Zunger, Phys. Rev. B **30**, 3430 (1984).

[90]A. Zunger, in *Solid State Physics*, edited by H. Ehrenreich, F. Seitz, and D. Turnbull (Academic, New York, 1986), Vol. 39, p. 275.

[91]D. S. McClure, in *Solid State Physics*, edited by H. Ehrenreich, F. Seitz, and D. Turnbull (Academic, New York, 1959), Vol. 8, p. 1; Vol. 9, p. 400.

[92]B. N. Figgis, *Introduction to Ligand Fields* (Interscience, New

York, 1966).
[93]J. C. Phillips, Rev. Mod. Phys. **42**, 317 (1970).
[94]T. M. Dunn, Trans. Faraday Soc. **57**, 1441 (1961).
[95]A. D. Liehr and C. J. Ballhausen, Ann. Phys. (N.Y.) **6**, 134 (1959).
[96]B. Müller, G. Roussos, and H.-J. Schulz, J. Crystal Growth **72**, 360 (1985); **73**, 646E (1985).
[97]A. G. O'Neill, Thesis, University of St. Andrews, Fife, U.K. (1983).
[98]J. L. Birman, Phys. Rev. **121**, 144 (1961).
[99]H.-J. Schulz, Phys. Status Solidi **3**, 485 (1963).
[100]S. W. Biernacki, H.-J. Schulz, Phys. Status Solidi B **103**, K 163 (1981).
[101]A. G. O'Neill, J. W. Allen, Solid State Commun. **46**, 833 (1983).
[102]L. A. Hemstreet, Phys. Rev. B **22**, 4590 (1980).
[103]J. A. Majewski, Phys. Status Solidi B **108**, 663 (1981).
[104]S. W. Biernacki, Phys. Status Solidi B **118**, 525 (1983).
[105]J. M. Baranowski and P. Vogl, in *Proceedings of the Twelfth Conference on Physics of Semiconducting Compounds,* edited by Polska Akademia Nauk (Wroclaw, Ossolineum, 1983), p. 74.
[106]P. Vogl, Adv. Electronics & Electron Phys. **62**, 101 (1984).
[107]S. Jugessur, J.-Y. Savard, and R. Rai, Canad, J. Phys. **48**, 2221 (1970).
[108]W. C. Holton, M. de Wit, R. K. Watts, T. L. Estle, and J. Schneider, J. Phys. Chem. Solids **30**, 963 (1969).
[109]W. Wegener, Dissertation TH Aachen, KFA Jülich, 1970.
[110]S. S. Mitra and R. Marshall, in *Proceedings of the Seventh International Conference on Semiconductors,* edited by M. Hulin (Dunod, Paris, 1964), p. 1085.
[111]R. Kuhnert and R. Helbig, J. Lumin. **26**, 203 (1981).
[112]Preliminary results of the present work have been presented in the following: (i) H.-J. Schulz, M. Thiede, *International Conference on Defects in Insulating Crystals* (University of Utah, Salt Lake City 1984), p. 413-414. (ii) H.-J. Schulz, M. Thiede, *Fifth General Conference of the Condensed Matter Division of the Europhysical Society* (Technische Universität, Berlin, 1985).